

An Adaptive, Multivariate Partitioning Algorithm for Global Optimization of Nonconvex Programs

Harsha Nagarajan · Mowen Lu · Site Wang · Russell Bent · Kaarthik Sundar

Received: date / Accepted: date

Abstract In this work, we develop an adaptive, multivariate partitioning algorithm for solving mixed-integer nonlinear programs (MINLP) with multi-linear terms to global optimality. The algorithm combines two key ideas that exploit the structure of convex relaxations to MINLPs. First, we apply sequential bound tightening techniques to obtain the tightest possible bounds, based on both continuous and discrete relaxations with partitioned variable domains. Second, we leverage relaxations to adaptively partition variable domains via piecewise convex relaxations of multi-linear terms and develop an iterative algorithm for globally solving MINLPs and provide proofs on convergence guarantees. We demonstrate the effectiveness of our disjunctive formulations and the algorithm on well-known benchmark problems (including Pooling and Blending instances) from MINLPLib and compare with a state-of-the-art global optimization solver. With this novel approach, we solve several large-scale instances which are, in some cases, intractable by the global optimization solver. We also shrink the best known optimality gap for one of the hard, generalized pooling problem instance.

1 Introduction

Mixed Integer Nonlinear Programs (MINLPs) are non-convex, mathematical programs that include discrete variables and nonlinear terms in the objective function and constraints. In practice, MINLPs arise in many applications such as chemical engineering (synthesis of process and water networks) [34,

Harsha Nagarajan · Russell Bent · Kaarthik Sundar
Center for Nonlinear Studies, Los Alamos National Laboratory
E-mail: {harsha, rbent, kaarthik}@lanl.gov

Mowen Lu · Site Wang
Department of Industrial Engineering, Clemson University
E-mail: {mlu87, sitew}@g.clemson.edu

45], energy infrastructure networks [22,31,41], and in molecular distance geometry problems [30]. In order to find global optimal solutions for MINLPs, non-convex terms are typically replaced with rigorous convex under- and over-estimators to obtain tight lower bounds. To this end, there has been a great deal of interest in the literature on developing function-specific convex estimators and hybrid relaxation strategies [7]. Further, in conjunction with branch-and-bound-type algorithms, the lower-bounding problems are tightened until a global optimum is obtained. With respect to implementations, these hybrid strategies have been dominant in solvers such as BARON [47], Couenne [5] and SCIP [1]. Despite major developments in the literature, MINLPs still remain difficult to solve and global optimization solvers often struggle to obtain optimal solutions and at times, even a feasible solution. The source of the difficulty is due to the weak, convex relaxations to the non-convex structures of the MINLP. Hence, in this paper we develop approaches that strengthen the convex relaxations of MINLP and use those relaxations to improve the performance of global solution techniques. We then test the effectiveness of the approach on MINLPs with multi-linear terms. These problems include well-known benchmark problems (including Pooling and Blending instances [28]) from MINLPlib. Our results are compared with state-of-the-art global optimization approaches. Our approach is able to significantly shrink the best-known optimality gaps on many instances, including a hard Pooling instance.

This paper makes three key contributions to solving MINLPs. First, variable bounds are a critical contributor to the quality of relaxations and ease of solving MINLPs to global optimality. As a result, bound-tightening methods have received a great deal of attention [12,4,11,17,38]. In the literature of global optimization, a simplified version of this procedure is usually referred to as “optimality-based bound contraction”, which involves a single iteration of solving minimization and maximization problems (convex) on every (or subset of) variable(s) [12,42]. Since this does not guarantee the tightest possible bounds on the variables, recent works have observed the effectiveness of (problem specific) sequential bound-tightening procedure in the context of various applications [14,39,55,40]. In this paper, we make the contribution of iteratively refining the bounds until the bounds converge to a fixed point on general MINLPs. Moreover, rather than solving convex minimization and maximization problems, this approach solves *discrete* minimization and maximization problems. Though this approach is counter-intuitive, computational experiments indicate that the value of the strengthened bounds from a discrete formulation often outweigh the computational time required to derive them.

The second contribution is focused on reducing the size of relaxed feasible regions. This is often done with domain partitioning. In multi-linear (and other) relaxations, many approaches build uniform, piecewise relaxations via univariate or bivariate partitioning [12,20,26,28]. This has also been a standard procedure applied in state-of-the-art global solvers. Uniform-partitioning method has particularly gained a lot of interest since this procedure also guarantees to obtain tight lower bounds by minimizing the least-square error from the non-convex function to the farthest point on the convex envelop on every

partition [20]. However, as the refinement procedure progresses on variables with large bounds, one of the drawbacks of such approaches is that they may need a large number of partitions that are controlled by on/off binary variables. As these binary variables introduce combinatorial explosion, these approaches are often restricted to small problems or limited domain partitions. As a result, recent work has focused on addressing these inefficiencies. For example, [11,13] combines multiparametric disaggregation with optimality-based bound contraction methods. In [54], the authors discuss a non-uniform, bivariate partitioning approach that improves relaxations but provide results for a single, simple benchmark problem. More recently, in [20], the authors report the advantages of bivariate (as compared to univariate) partitioning, however they use partitions chosen at uniformly located grid points. Reference [51] discusses a univariate parametrization method that solves medium-sized benchmarks. However, none of these approaches address the key limitation of uniform partitioning, *partition density*, i.e. these methods introduce partitions in unproductive regions.

We address this limitation by introducing a novel approach that adaptively partitions the relaxations in regions of the search space that favor optimality. To the best of our knowledge, there is little or no work on methods for solving MINLPs with such sparse partitioning. The most similar approach that we are aware of is [6]. They dynamically add a partitioning point at the midpoint of an active partition or at the value of a relaxation. In contrast, our approach explicitly adds a narrow partition around the values of a good solution.

Our third contribution relates to the algorithm itself. Instead of embedding the adaptive relaxation directly into spatial branching (sBB, α BB) methods [50,48], we develop a lower bounding algorithm built on the adaptively partitioned domains, and formulated as mixed-integer linear/quadratic programs (MILP/MIQP). This approach solves a succession of piecewise relaxations, each with a finer partitioning resolution. The solutions to the relaxations are used to recover feasible solutions to the original MINLP. The algorithm terminates when the relaxed solution and the feasible solution converge (within a given tolerance). While this approach is not sBB, it is very closely related. Each iteration of our algorithm implicitly explores (iteratively larger) sub-portions of an sBB search tree.

A preliminary version of this work (without rigorous analysis) appeared in a conference paper [39]. In this paper, we focused on demonstrating that the adaptive partitioning of convex relaxations empirically resulted in tighter relaxations. Also, we observed the efficacy of the adaptive convex relaxation tightening method on a hard, gas network optimization problem, modeled as a MINLP with engineering constraints [55]. Given the preliminary applications and efficacy of this idea, here, we extend this work considerably by using the relaxations to support an algorithm that globally solves MINLPs very effectively. The remainder of this paper is organized as follows: Section 2 discusses the required notation, problem set-up, and reviews standard relaxations for bilinear and multi-linear terms. Section 3 discusses our Adaptive, Multivariate Partitioning Algorithm that improves bound tightening, piecewise relaxations, and

globally solving MINLPs with a few proofs of convergence guarantees. Section 4 illustrates the strength of the algorithms on benchmark MINLPs and Section 5 concludes the paper. Finally, we note that the algorithm's implementation is available for download upon request.

2 Definitions

Notation Here, we use lower and upper case for vector and matrix entries, respectively. Bold font refers to the entire vector or matrix. With this notation, $\|\mathbf{v}\|_2$ defines the ℓ^2 norm of vector $\mathbf{v} \in \mathbb{R}^n$. Given vectors $\mathbf{v}_1 \in \mathbb{R}^n$ and $\mathbf{v}_2 \in \mathbb{R}^n$, $\mathbf{v}_1 \cdot \mathbf{v}_2 = \sum_{i=1}^n v_{1i}v_{2i}$; $\mathbf{v}_1 + \mathbf{v}_2$ implies element-wise sums; and $\frac{\mathbf{v}_1}{\alpha}$ denotes the element-wise ratio between entries of \mathbf{v}_1 and the scalar α . Next, $z \in \mathbb{Z}$ represents an integer (variable/constant) and specifically $z \in \mathbb{B}$ represents a binary variable.

Problem Without loss of generality (w.l.o.g.), the problems considered in this paper are MINLPs with multi-linear (polynomial) functions. The general form of the problem, denoted as \mathcal{P} , is as follows:

$$\begin{aligned} \mathcal{P} : \quad & \underset{\mathbf{x}, \mathbf{y}}{\text{minimize}} && f(\mathbf{x}, \mathbf{y}) \\ & \text{subject to} && \mathbf{g}(\mathbf{x}, \mathbf{y}) \leq 0, \\ & && \mathbf{h}(\mathbf{x}, \mathbf{y}) = 0, \\ & && \mathbf{x}^L \leq \mathbf{x} \leq \mathbf{x}^U, \\ & && \mathbf{y} \in \{0, 1\}^m \end{aligned}$$

where, $f : \mathbb{R}^n \times \mathbb{B}^m \rightarrow \mathbb{R}$, $g_i : \mathbb{R}^n \times \mathbb{B}^m \rightarrow \mathbb{R}$ for $i = 1, \dots, G$ and $h_i : \mathbb{R}^n \times \mathbb{B}^m \rightarrow \mathbb{R}$ for $i = 1, \dots, H$ are multi-linear functions. We restrict f , \mathbf{g} and \mathbf{h} to factorable functions, *i.e.*, functions that are recursive sums and/or products of univariate functions. For the sake of clarity and w.l.o.g., neglecting the binary variables in the functions, f , \mathbf{g} or \mathbf{h} can assume the following form:

$$\sum_{t \in T} a_t \prod_{k \in K_t} x_k^{\alpha_k} \quad (1)$$

where, $a_t \in \mathbb{R}$ is a coefficient and $(\alpha_k \geq 1) \in \mathbb{Z}$ is an exponent value. \mathbf{x} and \mathbf{y} are vectors of continuous variables with box constraints $(\mathbf{x}^L, \mathbf{x}^U)$ and binary variables, respectively. \mathbf{x} and \mathbf{y} have dimension n and m , respectively. We use notation σ to denote a solution to \mathcal{P} , where $\sigma(\cdot)$ is the value of variable(s), \cdot , in σ and $f(\sigma)$ is the objective value of σ . Note that \mathcal{P} is an NP-hard combinatorial problem and typically requires enormous search trees to evaluate the global optimum solutions [25].

McCormick Relaxations The construction of convex under-estimators and concave over-estimators for multi-linear functions of type (1) plays a critical role in developing algorithms for globally solving \mathcal{P} . An important special case when $|K_t| \leq 2$ for every $t \in T$ and $\alpha_k = 1$ for every $k \in K_t$, reduces \mathcal{P} to a bilinear MINLP. Specifically, for a single bilinear term ($|T| = 1$), McCormick [33] proposed to relax the set

$$S_B \subset \mathbb{R}^3 = \{(x_i, x_j, \widehat{x}_{ij}) \in [x_i^L, x_i^U] \times [x_j^L, x_j^U] \times \mathbb{R} \mid \widehat{x}_{ij} = x_i x_j\}$$

with the following four inequalities:

$$\widehat{x}_{ij} \geq x_i^L x_j + x_j^L x_i - x_i^L x_j^L \quad (2a)$$

$$\widehat{x}_{ij} \geq x_i^U x_j + x_j^U x_i - x_i^U x_j^U \quad (2b)$$

$$\widehat{x}_{ij} \leq x_i^L x_j + x_j^U x_i - x_i^L x_j^U \quad (2c)$$

$$\widehat{x}_{ij} \leq x_i^U x_j + x_j^L x_i - x_i^U x_j^L \quad (2d)$$

Let $\langle x_i, x_j \rangle^{MC} \supset S_B$ represent the feasible region defined by (2). For a single bilinear term $x_i x_j$, the relaxations in (2) describe the convex hull of set S_B [2]. We note that these relaxations can be strengthened when certain conditions are met. For example, [21] derives tighter relaxations based on perspective envelopes when the original non-convex set is described by $S_B^1 \subset \mathbb{R}^3 = \{(x_i, x_j, \widehat{x}_{ij}) \in [x_i^L, x_i^U] \times [x_j^L, x_j^U] \times \mathbb{R} \mid x_i \leq x_j, \widehat{x}_{ij} = x_i x_j\}$. Further, for the set $S_B^2 \subset \mathbb{B}^3 = \{(x_i, x_j, \widehat{x}_{ij}) \in \mathbb{B} \times \mathbb{B} \times \mathbb{B} \mid \widehat{x}_{ij} = x_i x_j\}$, it is trivial to observe that the relaxations in (2) are exact [19].

McCormick Relaxations of Multi-Linear Terms For a general factorable function with multi-linear terms ($|K_t| \geq 3$), McCormick proposed a recursive approach to successively derive envelopes on bilinear combinations of the terms (as described earlier). The resulting relaxation has formed the basis for the relaxations used in the global optimization literature, including the implementations in BARON, Couenne and SCIP [47, 5, 1]. More formally, the non-convex function given by $\prod_{k=1}^{|K_t|} x_k$ can be relaxed by constructing a higher-dimensional space by introducing lifted variables $\widehat{x}_1, \dots, \widehat{x}_{|K_t|-1}$ such that $\widehat{x}_1 = x_1 x_2$ and $\widehat{x}_i = \widehat{x}_{i-1} x_{i+1}$ for every $i = 2, \dots, |K_t| - 1$. Thus, recursive McCormick envelopes of $\prod_{k=1}^{|K_t|} x_k$ are described by

$$\{(x_1, x_2, \widehat{x}_1) \in [x_1^L, x_1^U] \times [x_2^L, x_2^U] \times [\widehat{x}_1^L, \widehat{x}_1^U] \mid \widehat{x}_1 = \langle x_1, x_2 \rangle^{MC}\}, \quad (3a)$$

$$\{(\widehat{x}_{i-1}, x_{i+1}, \widehat{x}_i) \in [\widehat{x}_{i-1}^L, \widehat{x}_{i-1}^U] \times [x_{i+1}^L, x_{i+1}^U] \times [\widehat{x}_i^L, \widehat{x}_i^U] \mid \widehat{x}_i = \langle \widehat{x}_{i-1}, x_{i+1} \rangle^{MC}\}, \quad \forall i = 2, \dots, |K_t| - 1. \quad (3b)$$

where, the bounds of \widehat{x}_i variables are derived appropriately. By abuse of notation, (3) can be succinctly represented as

$$\left\langle \prod_{k=1}^{|K_t|} x_k \right\rangle^{MC} = \left\langle \left\langle \langle x_1, x_2 \rangle^{MC}, \dots, x_{|K_t|-1} \right\rangle^{MC}, x_{|K_t|} \right\rangle^{MC}.$$

For a given single multi-linear term with generic bounds, the recursive McCormick envelopes described in (3) may not be the tightest relaxation and depends on the choice of recursion order in the space of original variables [49, 9]. However, authors in [46] prove that (3) indeed describes the convex hull when the bounds on the variables are $[0,1]$. This result on the description of convex hull was further generalized by [32] when the bounds on the variables are $[-U_i, U_i]$ (symmetric about the origin). More generally, multi-linear terms can also be relaxed using their convex hull characterization based on extreme points [43], which is usually not tractable due to the exponential growth in the number of variables.

Piecewise McCormick relaxations McCormick relaxations can be tightened by partitioning the bounds of the variables of multi-linear terms (see Figure 1[a]). As the number of partitions goes to ∞ , partitioning exactly approximates the original multi-linear terms. However, introducing a large number of partitions generally renders the problem intractable because the choice of partition is controlled by binary on/off variables. Given a bilinear term $x_i x_j$ and partition sets \mathcal{I}_i and \mathcal{I}_j , binary variables $\hat{\mathbf{y}}_i \in \{0,1\}^{|\mathcal{I}_i|}$ and $\hat{\mathbf{y}}_j \in \{0,1\}^{|\mathcal{I}_j|}$ are used to denote these partitions. Each entry in \mathcal{I}_i is pair of values, $\langle i, j \rangle$ that model the upper and lower bound of a variable in a partition. We refer to the collection of all partition sets with \mathcal{I} . These binary variables are used to control the partitions that are active and the associated relaxation of the active partition. Formally, the piecewise McCormick constraints, denoted by $\widehat{x}_{ij} \in \langle x_i, x_j \rangle^{MC(\mathcal{I})}$, take the following form:

$$\widehat{x}_{ij} \geq (\mathbf{x}_i^l \cdot \hat{\mathbf{y}}_i) x_j + (\mathbf{x}_j^l \cdot \hat{\mathbf{y}}_j) x_i - (\mathbf{x}_i^l \cdot \hat{\mathbf{y}}_i)(\mathbf{x}_j^l \cdot \hat{\mathbf{y}}_j) \quad (4a)$$

$$\widehat{x}_{ij} \geq (\mathbf{x}_i^u \cdot \hat{\mathbf{y}}_i) x_j + (\mathbf{x}_j^u \cdot \hat{\mathbf{y}}_j) x_i - (\mathbf{x}_i^u \cdot \hat{\mathbf{y}}_i)(\mathbf{x}_j^u \cdot \hat{\mathbf{y}}_j) \quad (4b)$$

$$\widehat{x}_{ij} \leq (\mathbf{x}_i^l \cdot \hat{\mathbf{y}}_i) x_j + (\mathbf{x}_j^l \cdot \hat{\mathbf{y}}_j) x_i - (\mathbf{x}_i^l \cdot \hat{\mathbf{y}}_i)(\mathbf{x}_j^l \cdot \hat{\mathbf{y}}_j) \quad (4c)$$

$$\widehat{x}_{ij} \leq (\mathbf{x}_i^u \cdot \hat{\mathbf{y}}_i) x_j + (\mathbf{x}_j^u \cdot \hat{\mathbf{y}}_j) x_i - (\mathbf{x}_i^u \cdot \hat{\mathbf{y}}_i)(\mathbf{x}_j^u \cdot \hat{\mathbf{y}}_j) \quad (4d)$$

$$\sum_{k=1}^{|\mathcal{I}_i|} \hat{y}_{i_k} = 1, \quad \sum_{k=1}^{|\mathcal{I}_j|} \hat{y}_{j_k} = 1 \quad (4e)$$

$$\hat{\mathbf{y}}_i \in \{0,1\}^{|\mathcal{I}_i|}, \quad \hat{\mathbf{y}}_j \in \{0,1\}^{|\mathcal{I}_j|} \quad (4f)$$

where, $(\mathbf{x}_i^l, \mathbf{x}_i^u) \in \mathcal{I}_i$ are the vector form of the partition sets of x_i (\mathcal{I}_i). Note that the bilinear terms in $\hat{\mathbf{y}}_j x_i$ and $\hat{\mathbf{y}}_i x_j$ are exactly linearized using standard McCormick relaxations. Also, $(\mathbf{x}_i^l \cdot \hat{\mathbf{y}}_i)(\mathbf{x}_j^l \cdot \hat{\mathbf{y}}_j)$ is rewritten as $\mathbf{x}_i^l (\hat{\mathbf{y}}_i \hat{\mathbf{y}}_j^T) \mathbf{x}_j^l$, where $\widehat{\mathbf{Y}} = (\hat{\mathbf{y}}_i \hat{\mathbf{y}}_j^T)$ is a matrix with binary product entries.

It is then straightforward to generalize piecewise McCormick relaxations to multilinear terms, and we use this notation to denote these relaxations

$$\left\langle \prod_{k=1}^{|\mathcal{K}_t|} x_k \right\rangle^{MC(\mathcal{I})} = \left\langle \left\langle \langle x_1, x_2 \rangle^{MC(\mathcal{I})}, \dots, x_{|\mathcal{K}_t|-1} \right\rangle^{MC(\mathcal{I})}, x_{|\mathcal{K}_t|} \right\rangle^{MC(\mathcal{I})} .$$

We also note that the unpartitioned McCormick relaxation is a special case of the partitioned McCormick relaxation where $\mathcal{I}_i = \{\langle x_i^L, x_i^U \rangle\}$.

These relaxations can also be encoded using $\log(|\mathcal{I}_i|)$ binary variables [16, 29, 53] or variations of special order sets (SOS1, SOS2). For an ease of exposition, we do not present the details of the log-based formulation in this paper. However, later in the results section, we do compare the effectiveness of SOS1 formulations with respect to the linear representation of binary variables.

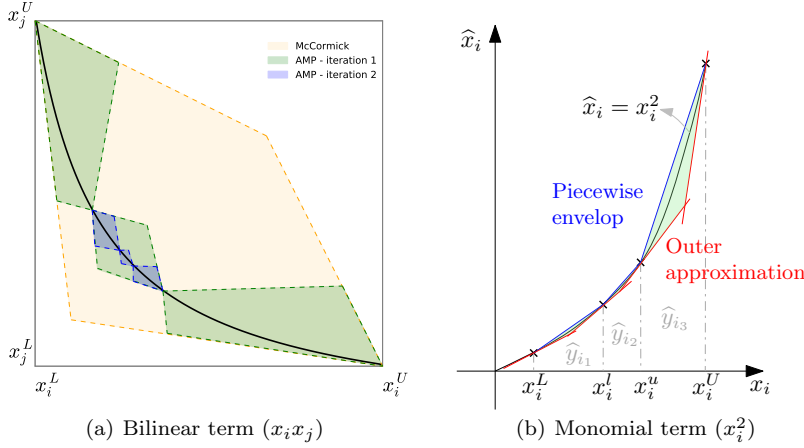


Fig. 1 Piecewise relaxations (shaded) of bilinear and monomial (quadratic) terms for a given set of partitions.

Piecewise Monomial Relaxations Without loss of generality¹, assume monomials take the form x_i^2 . Given partition \mathcal{I}_i , the piecewise, convex relaxation (see Figure 1[b]), denoted by $\hat{x}_i \in \langle x_i \rangle^{MC_q(\mathcal{I})}$, takes the form:

$$\hat{x}_i \geq x_i^2, \quad (5a)$$

$$\hat{x}_i \leq ((\mathbf{x}_i^L \cdot \hat{\mathbf{y}}_i) + (\mathbf{x}_i^U \cdot \hat{\mathbf{y}}_i)) x_i - (\mathbf{x}_i^L \cdot \hat{\mathbf{y}}_i)(\mathbf{x}_i^U \cdot \hat{\mathbf{y}}_i) \quad (5b)$$

$$\sum_{k=1}^{|\mathcal{I}_i|} \hat{y}_{ik} = 1 \quad (5c)$$

$$\hat{\mathbf{y}}_i \in \{0, 1\}^{|\mathcal{I}_i|} \quad (5d)$$

Once again, $(\mathbf{x}_i^L \cdot \hat{\mathbf{y}}_i)(\mathbf{x}_i^U \cdot \hat{\mathbf{y}}_i)$ is rewritten as $\mathbf{x}_i^L (\hat{\mathbf{y}}_i \hat{\mathbf{y}}_i^T) \mathbf{x}_i^U$, where $\hat{\mathbf{Y}} = (\hat{\mathbf{y}}_i \hat{\mathbf{y}}_i^T)$ is a symmetric matrix with binary product entries (squared binaries on diagonal). Hence it is sufficient to linearize the entries of the upper triangular matrix with

¹ In the case of higher order monomials, i.e., x_i^5 , apply a reduction of the form $x_i^2 x_i^2 x_i \Rightarrow \tilde{x}_i^2 x_i \Rightarrow \tilde{\tilde{x}}_i x_i$.

exact representations. We also note again that the unpartitioned relaxation is a special case where $\mathcal{I}_i = \{\langle x_i^L, x_i^U \rangle\}$.

Lemma 1 *The piecewise convex relaxation of $\langle x_i \rangle^{MC_q(\mathcal{I})}$ is strictly tighter than $\langle x_i, x_i \rangle^{MC(\mathcal{I})}$.*

Proof. Given \mathcal{I}_i for variable x_i , $\langle x_i, x_i \rangle^{MC(\mathcal{I})}$ reduces to the following three-inequalities:

$$\hat{x}_i \geq 2(\mathbf{x}_i^l \cdot \hat{\mathbf{y}}_i)x_i - (\mathbf{x}_i^l \cdot \hat{\mathbf{y}}_i)^2 \quad (6a)$$

$$\hat{x}_i \geq 2(\mathbf{x}_i^u \cdot \hat{\mathbf{y}}_i)x_i - (\mathbf{x}_i^u \cdot \hat{\mathbf{y}}_i)^2 \quad (6b)$$

$$\hat{x}_i \leq ((\mathbf{x}_i^l \cdot \hat{\mathbf{y}}_i) + (\mathbf{x}_i^u \cdot \hat{\mathbf{y}}_i))x_i - (\mathbf{x}_i^l \cdot \hat{\mathbf{y}}_i)(\mathbf{x}_i^u \cdot \hat{\mathbf{y}}_i) \quad (6c)$$

$$\sum_{k=1}^{|\mathcal{I}_i|} \hat{y}_{i_k} = 1, \quad (6d)$$

$$\hat{\mathbf{y}}_i \in \{0, 1\}^{|\mathcal{I}_i|}$$

Clearly, inequalities (6a) and (6b) are under-estimators of x_i^2 at all partition points in \mathcal{I}_i . The over-estimator in (6c) is the same as the over estimator defining $\langle x_i \rangle^{MC_q(\mathcal{I})}$. Further, the second-order conic under estimator of $\langle x_i \rangle^{MC_q(\mathcal{I})}$ can be equivalently described with infinitely many under-estimators. However, the under-estimators in $\langle x_i, x_i \rangle^{MC(\mathcal{I})}$ are finite, thus relaxing the set induced by the second-order-cone in $\langle x_i \rangle^{MC_q(\mathcal{I})}$. Therefore, $\langle x_i \rangle^{MC_q(\mathcal{I})} \subset \langle x_i, x_i \rangle^{MC(\mathcal{I})}$. Note that this proof can be also generalized to monomials with even exponents ($x_i^{2\alpha}$ for every $\alpha = 1, \dots, N$) \square

Given these definitions, we use $\mathcal{P}^{\mathcal{I}}$ to denote the relaxation of \mathcal{P} where all the multi-linear and monomial terms are replaced with the piecewise McCormick and monomial relaxations as defined by \mathcal{I} .

$$\begin{aligned} \mathcal{P}^{\mathcal{I}} : \quad & \underset{\mathbf{x}, \mathbf{y}}{\text{minimize}} && f^{\mathcal{I}}(\mathbf{x}, \mathbf{y}) \\ & \text{subject to} && \mathbf{g}^{\mathcal{I}}(\mathbf{x}, \mathbf{y}) \leq 0, \\ & && \mathbf{h}^{\mathcal{I}}(\mathbf{x}, \mathbf{y}) = 0, \\ & && \mathbf{x}_i^l \cdot \hat{\mathbf{y}}_i \leq x_i \leq \mathbf{x}_i^u \cdot \hat{\mathbf{y}}_i, \quad \forall i = 1 \dots n \\ & && \mathbf{y}, \hat{\mathbf{y}} \in \{0, 1\} \end{aligned}$$

where, $f^{\mathcal{I}}$, $\mathbf{g}^{\mathcal{I}}$ and $\mathbf{h}^{\mathcal{I}}$ inherit the above defined piecewise relaxations should the functions be nonlinear. It is important to note that while $\mathcal{P}^{\mathcal{I}}$ is defined in terms of piecewise relaxations on multi-linear terms. This definition of $\mathcal{P}^{\mathcal{I}}$ can be easily generalized to model other, possibly tighter and valid, (piecewise) relaxations and is a subject of future work. Also, we let $f^{\mathcal{I}}(\sigma)$ denote the objective value of a feasible solution, σ , to $\mathcal{P}^{\mathcal{I}}$.

3 Adaptive Multivariate Partitioning Algorithm

This section details the Adaptive Multivariate Partitioning (AMP) algorithm to compute global optimal solutions to MINLPs. The primary difference between the existing, MILP-based uniform partitioning approaches and AMP lies in the procedure that partitions the variable domains. In particular, AMP partitions the variable domains non-uniformly around the best-known, local-feasible solution.

The effectiveness of AMP also stems from the observation that the local optimal solutions found by the local solvers are often the globally optimal or are very close to the global optimal solution on standard benchmark instances. This observation has been previously made in the literature for optimal power flow problems in power grids [22,27]; optimal power flow problems can be modeled as NLPs with multi-linear terms and trigonometric functions. Also, the lower bounds obtained by solving the convex-quadratic/second-order conic relaxations were observed to be within 1% to 3% of the local-feasible solutions, further demonstrating the closeness of the local optimum solutions to its global counterpart. AMP exploits this structure and adds sparse, spatial partitions to the variable domains around the local-feasible solution. This partitioning scheme provides a degree-of-freedom for the MILP-based solver to (possibly) choose a tighter partition around the best-known local solution. Furthermore, it also adds discrete variables sparsely to the MILP used to lower bound the NLP that are independent of the size of the variable domains.

The pseudo-code of the describing the overall structure of AMP is given in Algorithm 1. The algorithm consists of two main components. The first component is a presolve (see lines 2 – 5). The presolve component of the algorithm is sub-divided into four parts: (i) computing an initial feasible solution, $\bar{\sigma}$, (line 2), (ii) creating an initial set of partitions, \mathcal{I} , (using the initial feasible solution obtained in line 2 if an initial feasible solve returns a solution), (iii) sequential bound-tightening (line 4), and (iv) computing an initial lower bound, $\underline{\sigma}$, using the relaxations detailed in Sec. 2 (line 5). The second component of AMP is the main loop (lines 6–11) that updates the upper bound, $\bar{\sigma}$, and the lower bound, $\underline{\sigma}$, of \mathcal{P} , until either of the following conditions are satisfied: the bounds are within ϵ or the solve times out. Apart from the aforementioned termination criteria, the algorithm would also terminate if the lower bounding solve is infeasible, implying \mathcal{P} is infeasible. At each iteration of the main loop, the partitions are refined and the corresponding piecewise convex relaxation is solved to obtain a lower bound (lines 7 and 8); similarly the upper bound is obtained using a local solver and updated if it is less than the best upper bound computed thus far (lines 9 and 10). In many ways, the partition step in line 7 can be thought of as implicitly searching iteratively larger portions of the spatial branch-and-bound search tree. In the following sections, we discuss each step of the algorithm in detail.

Algorithm 1 Adaptive Multivariate Partitioning (AMP) Algorithm

```

1: function AMP( $\mathcal{P}$ )
2:    $\bar{\sigma} \leftarrow \text{SOLVE}(\mathcal{P})$ 
3:    $\mathcal{I} \leftarrow \text{INITIALIZEPARTITIONS}(\mathcal{P}, \bar{\sigma})$ 
4:    $\mathbf{x}^l, \mathbf{x}^u \leftarrow \text{TIGHTENBOUNDS}(\mathcal{P}^{\mathcal{I}}, \bar{\sigma})$ 
5:    $\underline{\sigma} \leftarrow \text{SOLVE}(\mathcal{P}^{\mathcal{I}})$ 
6:   while  $\left(\frac{f(\bar{\sigma}) - f^{\mathcal{I}}(\underline{\sigma})}{f^{\mathcal{I}}(\underline{\sigma})} > \epsilon\right)$  and (Time < TimeOut) do
7:      $\mathcal{I} \leftarrow \text{TIGHTENPARTITIONS}(\mathcal{P}^{\mathcal{I}}, \underline{\sigma})$ 
8:      $\underline{\sigma} \leftarrow \text{SOLVE}(\mathcal{P}^{\mathcal{I}})$ 
9:      $\hat{\sigma} \leftarrow \text{SOLVE}(\mathcal{P}, \underline{\sigma})$ 
10:     $\bar{\sigma} \leftarrow \arg \min_{\sigma \in \bar{\sigma} \cup \hat{\sigma}} f(\sigma)$ 
11:  end while
12:  return  $\underline{\sigma}, \bar{\sigma}$ 
13: end function

```

3.1 Computing Feasible Solutions (Upper Bound)

A feasible solution, $\bar{\sigma}$, is computed for the first time in the presolve component of AMP (line 2). The initial feasible solution is computed by solving \mathcal{P} with a mixed-integer local solver (for instance, solvers that use primal-dual interior point methods in conjunction with a branch-and-bound search tree to handle integer variables). This feasible solution, $\bar{\sigma}$, is further used to initialize the partitions, \mathcal{I} (line 3). When the local solver reports infeasibility, we set $f(\bar{\sigma}) = \infty$ (line 4) and use the solution obtained by solving the unpartitioned convex (McCormick) relaxation of \mathcal{P} to initialize \mathcal{I} .

When the feasible solution computation step is invoked in the main loop of AMP (line 9), the feasible solution is obtained by solving the following NLP, \mathcal{P}^u , shown below. \mathcal{P}^u is constructed at each iteration of the main loop using the original MINLP, \mathcal{P} , and the lower bound solution computed at that iteration, $\underline{\sigma}$.

$$\mathcal{P}^u : \quad \underset{\mathbf{x}, \mathbf{y}}{\text{minimize}} \quad f(\mathbf{x}, \mathbf{y}) \quad (7a)$$

$$\text{subject to} \quad \mathbf{g}(\mathbf{x}, \mathbf{y}) \leq 0, \quad (7b)$$

$$\mathbf{h}(\mathbf{x}, \mathbf{y}) = 0, \quad (7c)$$

$$\mathbf{x}_i^l \cdot \underline{\sigma}(\hat{\mathbf{y}}_i) \leq x_i \leq \mathbf{x}_i^u \cdot \underline{\sigma}(\hat{\mathbf{y}}_i), \quad \forall i = 1 \dots n \quad (7d)$$

$$\mathbf{y} = \underline{\sigma}(\mathbf{y}) \quad (7e)$$

where the constraint (7d) forces the variable assignments into the partition defined by the current lower bound. The constraint (7e) fixes all the original binary variables to the lower bound solution. \mathcal{P}^u is then solved to local optimality using the a local solver. The motivation for this approach is based on empirical observations that the relaxed solution is often very near to the globally optimal solution and that the NLP is solved fast once all binary variables are fixed to constant values. \mathcal{P}^u is essentially a projection of the relaxed solution (lower bound solution, $\underline{\sigma}$) back onto a near point in the feasible region of \mathcal{P} ; this approach is often used for recovering feasible solutions [6].

3.2 Partition Initialization Scheme and Sequential Bound-Tightening

This section details the algorithm involved in lines 3 and 4 of the presolve component of AMP. The sequential bound-tightening procedure, defined in line 4 of Algorithm 1, is one of the key features of AMP. In many engineering applications there is little or no information about the upper and lower bounds ($\mathbf{x}^L, \mathbf{x}^U$) of these variables. Even when known, the gap between the bounds is often large. As discussed earlier in Sec. 2, these bounds are used in the relaxations to derive convex envelopes of non-convex terms in \mathcal{P} . Thus, large bounds generally weaken these relaxations, degrade the quality of the lower bounds, and slow down convergence. In practice, replacing the original bounds with tighter bounds can (sometimes) dramatically improve the quality of these relaxations. The basic idea of bound-tightening is the derivation of (new) valid bounds to improve the relaxations. Our approach is based on [12] and is related to the iterative bound-tightening of [14]. One of the key differences and innovations of our approach is that we use *mixed-integer models to shrink the bounds*. This is somewhat counter-intuitive as mixed-integer models are difficult to solve, but, when practical, much stronger, valid bounds are computed.

For the sequential bound-tightening part we present two procedures namely, bound-tightening without partitions (BT) and partition-based bound-tightening (PBT). The two procedures differ in the initial set of partitions, \mathcal{I} , used in the bound-tightening process. Hence, we first present two partition initialization schemes, one for the BT and another for the PBT, respectively. For bound-tightening without partitions, as the name suggests, the partition initialization scheme does not partition the variable domains *i.e.*, $\mathcal{I}_i \leftarrow \{x_i^L, x_i^U\}$ for every $i = 1, \dots, n$. In the case of PBT, the partition initialization scheme initializes three partitions around the local-feasible solution, $\bar{\sigma}$. This is done using an implementation of the function TIGHTENPARTITIONS (discussed in Section 3.4 and is also invoked in the main loop of AMP) on $\bar{\sigma}$. For the sake of completeness, a pseudo-code of the partition initialization function in line 3 is shown in Algorithm 2.

Once the initial set of partitions is computed based on the type of bound-tightening procedure, the sequential bound-tightening procedure computes new bounds by solving a modified version of $\mathcal{P}^{\mathcal{I}}$, given a continuous variable vector $\mathbf{x} \in \mathbb{R}^n$. First, for each x_i , a version of $\mathcal{P}^{\mathcal{I}}$ is solved where x_i is extremized, *i.e.*

$$\mathcal{P}_l^{\mathcal{I}}, \mathcal{P}_u^{\mathcal{I}} : \underset{\mathbf{x}, \mathbf{y}, \hat{\mathbf{y}}}{\text{minimize}} \pm x_i \quad (8a)$$

$$\text{subject to } f^{\mathcal{I}}(\mathbf{x}, \mathbf{y}) \leq f(\bar{\sigma}) \quad (8b)$$

$$\mathbf{g}^{\mathcal{I}}(\mathbf{x}, \mathbf{y}) \leq 0, \quad (8c)$$

$$\mathbf{h}^{\mathcal{I}}(\mathbf{x}, \mathbf{y}) = 0, \quad (8d)$$

$$\mathbf{x}_i^l \cdot \hat{\mathbf{y}}_i \leq x_i \leq \mathbf{x}_i^u \cdot \hat{\mathbf{y}}_i, \quad \forall i = 1 \dots n \quad (8e)$$

$$\mathbf{y}, \hat{\mathbf{y}} \in \{0, 1\} \quad (8f)$$

Algorithm 2 Partition Initialization Scheme

```

1: function INITIALIZEPARTITIONS( $\mathcal{P}, \bar{\sigma}$ )
2:   if Bound-tightening without partitions then
3:     for  $i \in 1 \dots n$  do
4:        $\mathcal{I}_i \leftarrow \{x_i^L, x_i^U\}$ 
5:     end for
6:     return  $\mathcal{I}$ 
7:   else
8:     if Partition-based bound-tightening then
9:       for  $i \in 1 \dots n$  do
10:         $\mathcal{I}_i \leftarrow \{x_i^L, x_i^U\}$ 
11:       end for
12:        $\mathcal{I} \leftarrow \text{TIGHTENPARTITIONS}(\mathcal{P}^{\mathcal{I}}, \bar{\sigma})$ 
13:       return  $\mathcal{I}$ 
14:     end if
15:   end if
16: end function

```

$\pm x_i$ in this formulation (8) denotes two optimization problems, where x_i and $-x_i$ are individually minimized. We refer to the problem of minimizing x_i and $-x_i$ as $\mathcal{P}_l^{\mathcal{I}}$ and $\mathcal{P}_u^{\mathcal{I}}$, respectively. In both cases, a constraint that bounds the original objective function of $\mathcal{P}^{\mathcal{I}}$ with a best known feasible solution $\bar{\sigma}$ (equation (8b)) is added when an initial feasible solution is available. This, combined with iterative bound-tightening, is another key difference between this approach and [12], [14]. More formally, Algorithm 3 describes the implementation of TIGHTENBOUNDS. The core of the algorithm is embedded in lines 3-10, where solutions to $\mathcal{P}_l^{\mathcal{I}}$ (line 6) and $\mathcal{P}_u^{\mathcal{I}}$ (line 7) are used to tighten bounds of each partition in \mathcal{I} (line 8). The procedure continues until the bounds do not change (line 3). Algorithm 3 is naturally parallel as each iteration of the for-loop (lines 5-9) is independently solvable.

Algorithm 3 Sequential bound-tightening of \mathbf{x}

```

1: function TIGHTENBOUNDS( $\mathcal{P}^{\mathcal{I}}, \bar{\sigma}$ )
2:    $\hat{\mathbf{x}}^l = \hat{\mathbf{x}}^u \leftarrow \mathbf{0}$ 
3:   while  $\|\mathbf{x}^l - \hat{\mathbf{x}}^l\|_2 > \epsilon$  &  $\|\mathbf{x}^u - \hat{\mathbf{x}}^u\|_2 > \epsilon$  do
4:      $\hat{\mathbf{x}}^l \leftarrow \mathbf{x}^l, \hat{\mathbf{x}}^u \leftarrow \mathbf{x}^u$ 
5:     for  $i=1, \dots, n$  do
6:        $\sigma_i^l \leftarrow \text{SOLVE}(\mathcal{P}_l^{\mathcal{I}})$ 
7:        $\sigma_i^u \leftarrow \text{SOLVE}(\mathcal{P}_u^{\mathcal{I}})$ 
8:        $\mathbf{x}_i^l \leftarrow \max(\sigma_i^l(x_i), \mathbf{x}_i^l), \mathbf{x}_i^u \leftarrow \min(\sigma_i^u(x_i), \mathbf{x}_i^u)$ 
9:     end for
10:   end while
11:   return  $\mathbf{x}^l, \mathbf{x}^u$ .
12: end function

```

Remark 1 Well-known bound-tightening procedures, usually referred to as domain reduction techniques in the global optimization literature [42, 24], is the

first iteration of the sequential procedure (BT) defined in Algorithm 3. Sequential bound tightening generalizes these techniques. Lemma 2 guarantees that Algorithm 3 converges to the tightest possible bounds for given $\mathcal{P}_l^{\mathcal{I}}$ and $\mathcal{P}_u^{\mathcal{I}}$.

Lemma 2 *For a given partition set \mathcal{I} with an associated (piecewise) convex relaxation and a feasible solution $\bar{\sigma}$ to \mathcal{P} , the sequential bound-tightening algorithm (BT/PBT) using the formulations $\mathcal{P}_l^{\mathcal{I}}$ and $\mathcal{P}_u^{\mathcal{I}}$ converges to the tightest possible variable bounds $[\mathbf{x}^l, \mathbf{x}^u]$ for a procedure based on minimizing and maximizing \mathbf{x} .*

Proof. Let k denote any iteration of the sequential bound-tightening algorithm, where each iteration constitutes solving $2n$ optimization problems ($\mathcal{P}_l^{\mathcal{I}}$ and $\mathcal{P}_u^{\mathcal{I}} \forall x_i, i = 1, \dots, n$). Also, let $[\mathbf{x}_k^l, \mathbf{x}_k^u]$ be the optimal bounds obtained at the k^{th} iteration of the algorithm. Then, for a fixed \mathcal{I} and $\bar{\sigma}$, the following observations are immediate: (1) the sequence of vectors $\{\mathbf{x}^l\}_k$ ($\{\mathbf{x}^u\}_k$) is a component-wise monotonically increasing (decreasing) sequence and (2) each value in the vector sequence $\{\mathbf{x}^l\}_k$ ($\{\mathbf{x}^u\}_k$) is bounded above (below) by a constant \mathbf{x}^U (\mathbf{x}^L). Note that \mathbf{x}^U and \mathbf{x}^L are the global bounds from \mathcal{P} . These two observations and monotone convergence theorem [10] together imply that these sequences converge to a unique limit $[\mathbf{x}^l, \mathbf{x}^u]$, proving the claim. \square

3.3 Lower Bound Computation

In lines 5 and 8, AMP generates solutions to the relaxed formulations, $\mathcal{P}^{\mathcal{I}}$. The objective value of these solutions are a lower bound to the global optimum. Line 5 computes the initial lower bound as a part of the presolve component of AMP and line 8 computes monotonically increasing lower bounds at each iteration of the main loop of AMP. Each $\mathcal{P}^{\mathcal{I}}$ is a mixed-integer, convex problem, where all the constraints are either linear or second-order cones (SOC). Theoretically, $\mathcal{P}^{\mathcal{I}}$ can be solved by off-the-shelf mixed-integer, second-order cone solvers. However, initial computational experiments suggested that several moderately sized problems with SOC constraints were difficult to solve, even with modern, state-of-the-art solvers. It was the case that either the solver convergence was very slow or the solve terminated with a numerical error. To circumvent this issue, a cutting-plane algorithm was implemented to outer-approximate the SOC constraints. This approach relaxes SOC constraints with a finite number of valid cutting planes (first order derivatives) that define an outer envelop and produces a lower bound on the optimal solution. This lower bound is tightened for every violated SOC constraint by adding corresponding valid cuts until the solution is feasible, and hence, optimal for the original SOC set. Figure 1(b) illustrates this outer-approximation procedure on monomial relaxations. Red colored lines are the under estimators of x_1^2 and the valid cutting planes added to the formulation. We expect the need for this technical detail to diminish as conic solvers improve.

3.4 Partition Tightening

One of the core contributions of the AMP algorithm is in the implementations of TIGHTENPARTITIONS. This part of the algorithm tightens the convex relaxations by discretizing the domains on non-convex terms. Many of the existing approaches assume a (small) finite number of partitions that uniformly discretize the variable space [18, 6, 12, 20]. While this is a straight-forward approach for partitioning the domain of variables, it potentially creates partitions that are far away from the optimality region of the search space *i.e.*, many of the partitions are not useful. Instead, our approach successively tightens the relaxations with sparse domain discretization. This approach focuses partitioning on regions of the variable domain that appear to influence optimality the most. These regions are defined by a solution σ that is typically an upper or lower bound (but could be any solution).

Algorithm 4 Dynamic partitioning of variable domains

```

1: function TIGHTENPARTITIONS-ADAPTIVE( $\mathcal{P}^{\mathcal{I}}, \sigma$ )
2:   for  $i \in 1 \dots n$  do
3:      $k \leftarrow \arg \max \sigma(\hat{y}_i^k)$ 
4:      $\langle l_i, u_i \rangle \leftarrow \mathcal{I}_i^k$ 
5:      $\xi_i \leftarrow \frac{u_i - l_i}{\Delta}$ 
6:     if  $\xi_i > \epsilon$  then
7:        $\gamma_1 \leftarrow \min(l_i, \max(\sigma(x_i) - \xi_i, x_i^L))$ 
8:        $\gamma_2 \leftarrow \max(l_i, \sigma(x_i) - \xi_i)$ 
9:        $\gamma_3 \leftarrow \min(u_i, \sigma(x_i) + \xi_i)$ 
10:       $\gamma_4 \leftarrow \max(u_i, \min(\sigma(x_i) + \xi_i, x_i^U))$ 
11:       $\mathcal{I}_i \leftarrow (\mathcal{I}_i \setminus \langle l_i, u_i \rangle) \cup \langle \gamma_1, \gamma_2 \rangle \cup \langle \gamma_2, \gamma_3 \rangle \cup \langle \gamma_3, \gamma_4 \rangle$ 
12:    else
13:       $\langle l_i, u_i \rangle \leftarrow \arg \max_{\mathcal{I}_i} u_i - l_i$ 
14:       $\mathcal{I}_i \leftarrow (\mathcal{I}_i \setminus \langle l_i, u_i \rangle) \cup \langle l_i, l_i + \frac{u_i - l_i}{2} \rangle \cup \langle l_i + \frac{u_i - l_i}{2}, u_i \rangle$ 
15:    end if
16:  end for
17:  return  $\mathcal{I}$ 
18: end function

```

Uniform Domain Partitioning For comparison purposes, TIGHTRELAXATION is also implemented to mimic the uniform partitioning approaches of [18, 6, 12, 20]. The implementation is defined in Algorithm 5. Every execution of this implementation doubles the number of partitions (line 3).

Adaptive Domain Partitioning The pseudo-code of the adaptive domain partition algorithm is outlined in Algorithm 4. For a variable x_i , the active partition is the partition whose \hat{y}_i variable takes a value of 1 (line 3) in a solution (σ). The active partition defines a lower bound and an upper bound for a choice of the value for x_i . The active partition is then split into three new partitions (lines 7-11). As shown in line 5 of Algorithm 4, the size of the new partition

Algorithm 5 Uniform partitioning of variable domains

```

1: function TIGHTENPARTITIONS-UNIFORM( $\mathcal{P}^{\mathcal{I}}, \sigma$ )
2:   for  $i \in 1 \dots n$  do
3:      $\mathcal{I}_i \leftarrow \bigcup_{\langle l_i, u_i \rangle \in \mathcal{I}_i} \left( \langle l_i, l_i + \frac{u_i - l_i}{2} \rangle \cup \langle l_i + \frac{u_i - l_i}{2}, u_i \rangle \right)$ 
4:   end for
5:   return  $\mathcal{I}$ 
6: end function

```

depends on the size of the active partition. The user parameter, $\Delta > 1$, is used to scale the partition's size and this in turn influences the rate of convergence and the number of partitions. Lines 13-14 split partitions outside the active partition when the active partition is too small and is used to ensure convergence. Figure 2 illustrates the successive partitioning that occurs at every execution of TIGHTENPARTITIONS on the variables of a bilinear term. Figure 1(a) geometrically illustrates the tightening of piecewise convex envelopes induced due to the iterative adaptive-partitioning scheme.

Lemma 3 Let $\underline{\sigma}^{\mathcal{I}}$ denote the optimal solution to the formulation $\mathcal{P}^{\mathcal{I}}$ and let σ^* denote the global optimal solution to \mathcal{P} . Then, $f^{\mathcal{I}}(\underline{\sigma}^{\mathcal{I}})$ monotonically increases to $f(\sigma^*)$ as $|\mathcal{I}_i| \rightarrow \infty$ for every $i = 1, \dots, n$.

Proof. Without loss of generality, we assume \mathcal{P} is feasible. Since \mathcal{P} consists only of factorable functions, again, without loss of generality, we restrict our discussion to bilinear terms. Let $x_i x_j$ be a bilinear term. Given a finite set of partitions, that is, $1 \leq |\mathcal{I}_i|, |\mathcal{I}_j| < \infty$, there always exists a partition in \mathcal{I}_i and \mathcal{I}_j that is active in the solution to $\mathcal{P}^{\mathcal{I}}$. Let the active partitions have lengths $\epsilon_i^l + \epsilon_i^u$ and $\epsilon_j^l + \epsilon_j^u$, respectively. Also, assume the active partition contains the global optimum solution $\sigma^*(\mathbf{x}^*, \mathbf{y}^*)^2$. Then, we have

$$x_i^* - \epsilon_i^l \leq x_i \leq x_i^* + \epsilon_i^u, \quad x_j^* - \epsilon_j^l \leq x_j \leq x_j^* + \epsilon_j^u.$$

For these active partitions, the McCormick constraints in (4a) and (4c) linearize $x_i x_j$ as follows:

$$\begin{aligned} \widehat{x}_{ij} &\geq (x_i^* - \epsilon_i^l)x_j + (x_j^* - \epsilon_j^l)x_i - (x_i^* - \epsilon_i^l)(x_j^* - \epsilon_j^l) \\ &= (x_i^*x_j + x_j^*x_i - x_i^*x_j^*) + \underbrace{\epsilon_i^l(x_j^* - x_j) + \epsilon_j^l(x_i^* - x_i) - \epsilon_i^l\epsilon_j^l}_{\mathcal{E}(\epsilon_i^l, \epsilon_j^l)} \end{aligned} \quad (9)$$

and

$$\begin{aligned} \widehat{x}_{ij} &\leq (x_i^* - \epsilon_i^l)x_j + (x_j^* + \epsilon_j^u)x_i - (x_i^* - \epsilon_i^l)(x_j^* + \epsilon_j^u) \\ &= (x_i^*x_j + x_j^*x_i - x_i^*x_j^*) + \underbrace{\epsilon_i^l(x_j^* - x_j) + \epsilon_j^u(x_i - x_i^*) + \epsilon_i^l\epsilon_j^u}_{\mathcal{E}(\epsilon_i^l, \epsilon_j^u)} \end{aligned} \quad (10)$$

² At a given iteration, the active partition may not contain the global optimal. However, by lines 13 and 14 in Algorithm 4 AMP, AMP will eventually partition all other domains small enough such that in an iteration, AMP will pick an active partition with the global optimal whose length is $\leq \epsilon_i^l + \epsilon_i^u$.

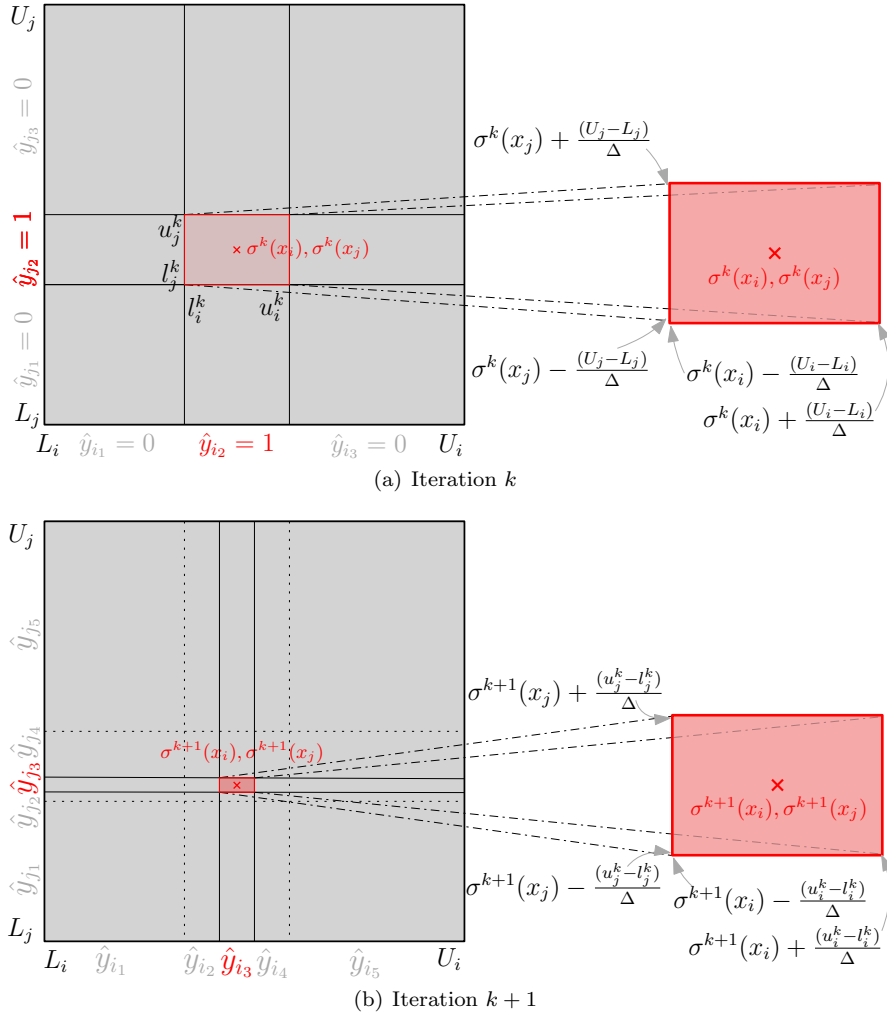


Fig. 2 Adaptive partitioning strategy for a bilinear function $x_i x_j$ as described in Algorithm 4. Red and gray colored boxes represent active and inactive partitions, respectively. k and $k + 1$ refer to successive solutions used to partition the active partition.

where, $\mathcal{E}(\epsilon_i^l, \epsilon_j^l) < 0$ and $\mathcal{E}(\epsilon_i^u, \epsilon_j^u) > 0$ are the error terms of the under- and over-estimator, respectively. It is trivial to observe that the error terms themselves constitute the McCormick envelopes of $(x_i^* - x_i)(x_j^* - x_j)$ if one were to linearize this product.

Uniform partitioning case: In this case, for $|\mathcal{I}_i|$ and $|\mathcal{I}_j|$, the length of the active partition that contains the global solution is

$$\epsilon_i^l + \epsilon_i^u = \frac{U_i - L_i}{|\mathcal{I}_i|}, \quad \epsilon_j^l + \epsilon_j^u = \frac{U_j - L_j}{|\mathcal{I}_j|}$$

Adaptive partitioning case: In this case, line 7 in Algorithm 1 ensures that the partitions created during the $(k+1)^{th}$ iteration of the main loop for either of the variables, x_i or x_j , is a subset of the partitions created for the corresponding variables in the k^{th} iteration. Also, for a k^{th} iteration of an adaptive refinement step for variables x_i and x_j , we assume that at most $3 + 2(k - 1)$ partitions exist within the given variable bounds (L_i, U_i) and (L_j, U_j) , respectively. Thus, the length of the above mentioned active partition which contains the global solution is given by

$$\epsilon_i^l + \epsilon_i^u = \frac{U_i - L_i}{\Delta^{\frac{|\mathcal{I}_i|-1}{2}}}, \quad \epsilon_j^l + \epsilon_j^u = \frac{U_j - L_j}{\Delta^{\frac{|\mathcal{I}_j|-1}{2}}}.$$

For either of the above cases, clearly as $|\mathcal{I}_i|$ and $|\mathcal{I}_j|$ approach ∞ , the error terms of the McCormick envelopes, $\mathcal{E}(\epsilon_i^l, \epsilon_j^l)$ and $\mathcal{E}(\epsilon_i^l, \epsilon_j^u)$, approach zero, and thus enforcing $x_i = x_i^*$, $x_j = x_j^*$ and $\widehat{x}_{ij} = x_i^* x_j^*$. Therefore, as $|\mathcal{I}_i|$ approaches ∞ for every variable i that is being partitioned, $f^{\mathcal{I}}(\sigma^{\mathcal{I}})$ approaches the global optimal solution $f(\sigma^*)$.

Also observe that since the $\mathfrak{F}(\mathcal{P}^{\mathcal{I}}) \subset \mathfrak{F}(\mathcal{P})$ for any finite \mathcal{I} , $f^{\mathcal{I}}(\sigma^{\mathcal{I}}) \leq f(\sigma^*)$. Furthermore, the partition set in iteration k is a proper subset of the previous iteration's partitions. This proves the monotonicity of the sequence of values $f^{\mathcal{I}}(\sigma^{\mathcal{I}})$ with increasing iterations of the main loop of AMP. \square

Lemma 4 Let $[\mathbf{x}^l, \mathbf{x}^u]$ represent the tightened bounds obtained from lines 3 and 4 of Algorithm 1. Then, the global optimum $\sigma(\mathbf{x}^*)$ of \mathcal{P} is contained in $[\mathbf{x}^l, \mathbf{x}^u]$.

Proof. Since BT is a special case of PBT, without loss of generality, we prove the result for PBT. For any initial set of partitions computed by the partition initialization scheme, \mathcal{I} , we have $\mathfrak{F}(\mathcal{P}) \subset \mathfrak{F}(\mathcal{P}^{\mathcal{I}})$, where $\mathfrak{F}(\cdot)$ denotes the feasible space of the formulation. Now, consider the constraint (8b). Observe that the right hand side of the constraint (8b) is the objective value of the solution obtained using the local solver and hence, (8b) is guaranteed to not remove the global optimal solution to \mathcal{P} . Hence, we have $\mathfrak{F}(\mathcal{P} \cup (8b)) \subset \mathfrak{F}(\mathcal{P}^{\mathcal{I}} \cup (8b)) = \mathfrak{F}(\mathcal{P}_l^{\mathcal{I}}) = \mathfrak{F}(\mathcal{P}_u^{\mathcal{I}})$. But, the PBT computes the tightest bounds on each variable on the region defined by $\mathfrak{F}(\mathcal{P}_l^{\mathcal{I}})$, $\mathfrak{F}(\mathcal{P}_u^{\mathcal{I}})$. Hence, the tightened bounds, $[\mathbf{x}^l, \mathbf{x}^u]$, obtained after PBT is valid for $\mathfrak{F}(\mathcal{P}_l^{\mathcal{I}})$, $\mathfrak{F}(\mathcal{P}_u^{\mathcal{I}})$, implying that it is valid for $\mathfrak{F}(\mathcal{P} \cup (8b))$. Hence, enforcing these tightened bounds on $\mathfrak{F}(\mathcal{P})$ does not remove the global optimal solution of \mathcal{P} . \square

4 Computational results

In remainder of this paper, we refer to AMP as Algorithm 1 without the implementation of lines 3 and 4, *i.e.*, without any form of bound-tightening. BT-AMP and PBT-AMP refer to Algorithm 1 implemented with bound-tightening with and without partitions added, respectively. The performance of these algorithms is evaluated on a set of standard benchmarks from the literature

with multi-linear terms. These problems include a small NLP that is used to highlight the differences between the AMP algorithm and uniform partitioning approaches. The details and sources for each problem instance chosen are shown later in this section in Table 7. In this table, we also mention the continuous variables in multi-linear terms chosen for partitioning³. Ipopt 0.2.6 and Bonmin are used as local NLP and MINLP solvers for the feasible solution computation in AMP, respectively. MILPs and MIQCQCPs are solved using CPLEX 12.7 (cpx) and/or Gurobi 7.0.2 (grb) with default options and presolver switched on. These two solvers were chosen because they are the most advanced mixed-integer convex quadratic solvers; we also remark that the performance of these solvers vary based on the instance chosen and its respective relaxations. The outer-approximation algorithm was implemented using the lazy callback feature of CPLEX and Gurobi. Given that the bound-tightening procedure consists of independently solvable problems, 10 parallel threads were used during bound-tightening. In the Appendix we provide a detailed sensitivity analysis of the parameters of AMP.

Every bound-tightening (BT and PBT) problem was solved to optimality (except *meyer15*). For *meyer15*, 0.1% optimality gap was used as a termination criteria because it is a large-scale MINLP⁴. The value of ϵ and the “TimeOut” parameter in Algorithm 1 were set to 0.0001 and 3600 seconds, respectively. However, for BT and PBT, we did not impose any time limit. Thus, for a fair comparison, we set the time limit of the comparison global solver to the sum of bound tightening time and 3600 seconds (denoted by T^+ in the tables). In the results, “TO” indicates that the AMP solve timed-out. All results are benchmarked with BARON 17.1, a state-of-the-art global optimization solver [47,50]. CPLEX 12.7 and Ipopt 0.2.6 are used as the underlying MILP and non-convex local solvers for BARON. JuMP, an algebraic modeling language in Julia [15], was used for implementing all the algorithms and invoking the optimization solvers. All the computational experiments were performed using the high-performance computing resources at the Los Alamos National Laboratory with Intel CPU E5-2660-v3, Haswell micro-architecture, 20 cores (2 threads per core) and 125GB of memory.

4.1 Performance on a Small-scale NLP

In this section, we perform a detailed study of AMP with and without bound-tightening on *NLP1*, a small-scale, continuous nonlinear program adapted from Problem 106 in [23]. This small problem helps illustrate many of the salient features of AMP. *NLP1* has gained considerable interest from the global optimization literature due its large variable bounds and weak McCormick relaxations. Since this is a challenging problem for uniform, piecewise McCormick relaxations, this problem has been studied in detail in [12,11,51]. The value of the

³ See [7] for more details on strategies for choosing the variables for partitioning.

⁴ The bounds are computed using the best lower bound of \mathcal{P}_l^Z and the best upper bound of \mathcal{P}_u^Z maintained by the solver.

global optimum for $NLP1$ is 7049.2479 and the solution is x_i^* , $i = 1, \dots, 8 = [579.307, 1359.97, 5109.97, 182.018, 295.601, 217.982, 286.417, 395.601]$.

$$\begin{aligned}
 NLP1 : \quad & \underset{x_1, \dots, x_8}{\text{minimize}} && x_1 + x_2 + x_3 \\
 & \text{subject to} && 0.0025(x_4 + x_6) - 1 \leq 0, \\
 & && 0.0025(-x_4 + x_5 + x_7) - 1 \leq 0, \\
 & && 0.01(-x_5 + x_8) - 1 \leq 0, \\
 & && 100x_1 - x_1x_6 + 833.33252x_4 - 83333.333 \leq 0, \\
 & && x_2x_4 - x_2x_7 - 1250x_4 + 1250x_5 \leq 0, \\
 & && x_3x_5 - x_3x_8 - 2500x_5 + 1250000 \leq 0, \\
 & && 100 \leq x_1 \leq 10000, \\
 & && 1000 \leq x_2, x_3 \leq 10000, \\
 & && 10 \leq x_4, x_5, x_6, x_7, x_8 \leq 1000
 \end{aligned}$$

4.1.1 AMP versus Uniform Partitioning on $NLP1$

Figure 3 compares AMP (without BT/PBT) with a uniform partitioning strategy that is often used in state-of-the-art solvers to obtain global solutions. For a fair comparison, we used the same number of partitions for both methods at every iteration. From Figure 3(a), it is evident that AMP exhibits larger optimality gaps in the first few iterations (134%, 44%, 20%, vs. 97%, 44%, 16%, etc.). However, the convergence rate to global optimum is much faster with AMP (within 190.9 seconds). This behaviour is primarily attributed to the adaptive addition of partitions around the best-known local solution (also global in this case) instead of spreading them uniformly.

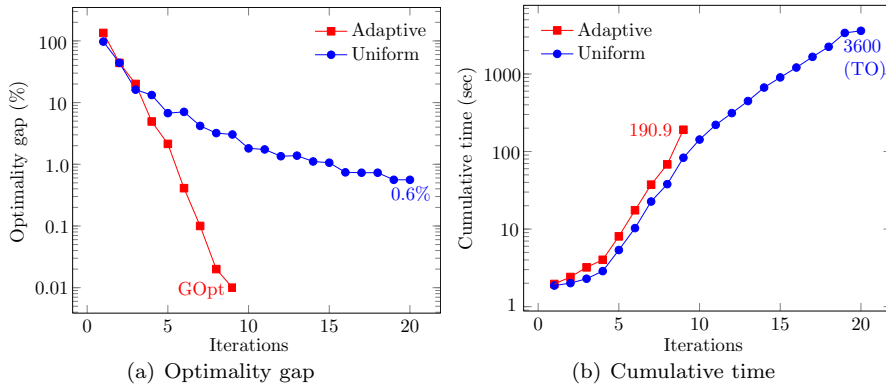


Fig. 3 Performance of AMP ($\Delta = 4$) and uniform partitioning on $NLP1$. Note that the y-axis is on log scale.

4.1.2 Performance of AMP on NLP1

Figure 4 shows the active partitions chosen by every iteration of AMP for $\Delta = 4$. This figure illustrates the active partitions at each iteration of the main loop of AMP and the convergence of each variable partition to its corresponding global optimal value. One of the primary motivations of the adaptive partitioning strategy comes from the observation that every new partition added adaptively refines the regions (hopefully) closer to the global optimum values. In Figure 4(a), this behaviour is clearly evident on all the variables except x_3 . Although the initial active partition on x_3 did not contain the global optimum, AMP converged to the global optimum value. The convergence time of AMP to the global optimum using Gurobi was *190.9 seconds*. The total number of binary partitioning variables is 152 (19 per continuous variable).

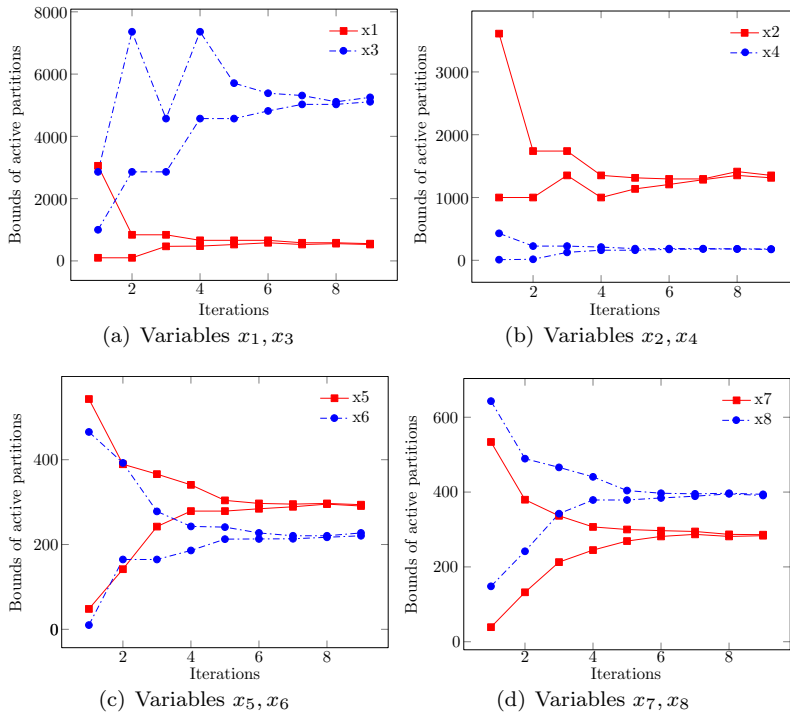


Fig. 4 Upper and lower bounds of active partitions chosen by AMP algorithm (without bound-tightening) for the variables $x_i, i = 1, \dots, 8$ of *NLP1*.

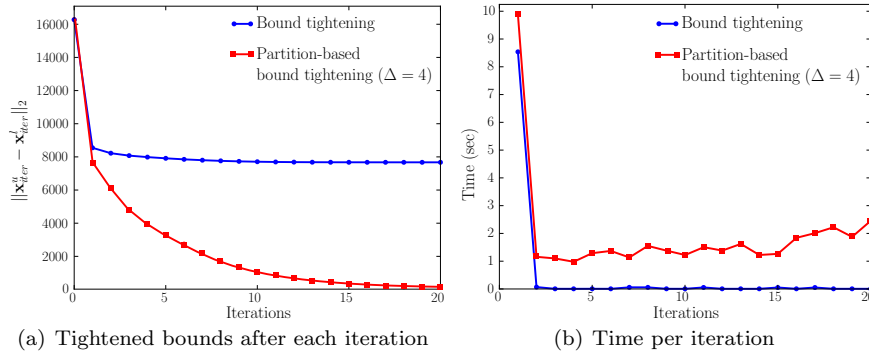


Fig. 5 Performance of sequential BT and sequential PBT techniques on *NLP1*.

4.1.3 Benefits of Bound-Tightening on *NLP1*

Figure 5 and Table 1 show the effectiveness of sequential BT and sequential PBT techniques on *NLP1*. As expected, in Figure 5(a), the disjunctive polyhedral representation of the relaxed regions in PBT (around the initial local solution) drastically reduce the global bounds on the variables (to almost zero gaps). Figure 5(b) shows that PBT, even when solving a MILP in every iteration, does not incur too much computational overhead on a small-scale problem like *NLP1*.

A qualitative description of the improved performance is presented in Table 1. The values shown under the column titled “PBT bounds” clearly show that PBT-AMP converges to global optimum values with an addition of very few binary variables (48) within 50 seconds. Overall, for *NLP1*, it is noteworthy that PBT-AMP outperforms most of the state-of-the-art piecewise relaxation methods developed in the literature.

Table 1 Contracted bounds after applying sequential bound tightening to nlp1.

Variable	Original bounds		PBT bounds		#BVars added	
	L	U	l	u	BT-AMP ($\Delta = 4$)	PBT-AMP ($\Delta = 4$)
x_1	100	10000	573.1	585.1	14	3+3
x_2	1000	10000	1351.2	1368.5	14	3+3
x_3	1000	10000	5102.1	5117.5	15	3+3
x_4	10	1000	181.5	182.5	15	3+3
x_5	10	1000	295.3	296.0	15	3+3
x_6	10	1000	217.5	218.5	15	3+3
x_7	10	1000	286.0	286.9	15	3+3
x_8	10	1000	395.3	396.0	15	3+3
Total					118	48

4.2 Performance of AMP on Large-scale MINLPs

Table 2 Summary of the performance of AMP without bound-tightening on all instances. Here, we compare the run times of BARON, AMP with $\Delta = 8$ (cpx), AMP with the best Δ (cpx) and AMP with the best Δ (grb). Values under “Gap” and “T” are in % and seconds, respectively. “Inf” implies that the solver failed to provide a bound within the prescribed time limit.

Instances	BARON		AMP-cpx $\Delta = 8$		AMP-cpx Δ^*			AMP-grb Δ^*		
	Gap	T	Gap	T	Δ	Gap	T	Δ	Gap	T
p1	GOpt	0.02	GOpt	0.26	32	GOpt	0.19	32	GOpt	0.06
p2	GOpt	0.01	GOpt	0.05	16	GOpt	0.03	32	GOpt	0.10
fuel	GOpt	0.03	GOpt	0.07	4	GOpt	0.03	4	GOpt	0.05
ex1223a	GOpt	0.02	GOpt	0.01	32	GOpt	0.01	16	GOpt	0.02
ex1264	GOpt	1.44	GOpt	1.42	16	GOpt	0.90	8	GOpt	0.79
ex1265	GOpt	13.30	GOpt	0.94	16	GOpt	0.17	8	GOpt	0.28
ex1266	GOpt	10.81	GOpt	0.27	32	GOpt	0.14	32	GOpt	0.16
eniplac	GOpt	207.37	GOpt	1.17	32	GOpt	0.68	32	GOpt	0.75
util	GOpt	0.10	GOpt	1.21	16	GOpt	0.54	16	GOpt	0.55
meanvarx	GOpt	0.05	GOpt	290.61	16	GOpt	95.51	16	GOpt	70.09
blend029	GOpt	2.46	GOpt	1.74	32	GOpt	0.74	32	GOpt	1.00
blend531	GOpt	111.79	GOpt	185.33	8	GOpt	185.33	16	GOpt	49.76
blend146	2.20	TO	2.01	TO	8	2.01	TO	8	1.60	TO
blend718	175.10	TO	GOpt	379.58	8	GOpt	379.58	8	GOpt	581.68
blend480	GOpt	326.95	0.32	TO	32	0.04	TO	16	0.02	TO
blend721	GOpt	548.90	GOpt	504.74	32	GOpt	256.77	16	GOpt	176.11
blend852	0.08	TO	GOpt	750.88	4	GOpt	169.24	16	GOpt	322.80
wtsM2_05	GOpt	153.30	20.08	TO	8	20.08	TO	32	GOpt	386.95
wtsM2_06	GOpt	228.18	8.76	TO	4	GOpt	2395.71	32	GOpt	972.20
wtsM2_07	GOpt	759.96	0.10	TO	8	0.10	TO	16	0.54	TO
wtsM2_08	388.62	TO	9.82	TO	4	5.45	TO	4	7.92	TO
wtsM2_09	Inf	TO	68.58	TO	10	36.47	TO	4	7.47	TO
wtsM2_10	76.48	TO	35.88	TO	32	24.95	TO	16	0.10	TO
wtsM2_11	107.56	TO	7.88	TO	16	3.50	TO	4	6.10	TO
wtsM2_12	85.35	TO	8.07	TO	4	7.46	TO	32	4.00	TO
wtsM2_13	54.04	TO	10.06	TO	4	4.24	TO	8	5.72	TO
wtsM2_14	46.24	TO	9.02	TO	32	6.34	TO	16	1.43	TO
wtsM2_15	Inf	TO	86.64	TO	4	8.81	TO	8	0.22	TO
wtsM2_16	47.77	TO	34.46	TO	8	34.46	TO	32	5.25	TO
lee1	GOpt	145.55	GOpt	13.01	8	GOpt	13.01	8	GOpt	13.61
lee2	GOpt	590.08	0.58	TO	16	0.47	TO	16	0.08	TO
meyer4	80.40	TO	GOpt	18.85	4	GOpt	12.50	8	GOpt	5.68
meyer10	239.70	TO	GOpt	TO	4	GOpt	452.53	8	GOpt	133.47
meyer15	2850.30	TO	0.59	TO	16	0.31	TO	4	0.10	TO

In this section we assess the empirical value of adaptive partitioning by presenting results without bound-tightening. In Table 2, AMP (without bound-tightening) with CPLEX or Gurobi is compared with BARON. Column two shows the run times of BARON based on the 3600 second time limit. Column three shows the performance of AMP for $\Delta = 8$. Though $\Delta = 8$ is not the ideal setting for every instance, it is analogous to running BARON with default parameters. Under the default AMP settings, AMP is faster than BARON (with default settings) at finding the best lower bound in 23 out of 34 instances. The notable exception to AMP’s performance is problem *p3*. For *p3*, the convergence of AMP is much slower than BARON. This is primarily due to the

large variable bounds and also highlights the need for bound-tightening in conjunction with adaptive partitioning.

In column four (tuned Δ and CPLEX), the run times of AMP are much faster than BARON in 24 out of 34 instances. It is interesting to observe on problem $p3$ that the run time is decreased by an order of magnitude with the right choice of Δ (bound-tightening improves it further). Column five (tuned Δ and Gurobi) again indicates that the right choice of Δ speeds up the convergence of AMP drastically. More interestingly, on 21 out of 34 instances, the run times of AMP using Gurobi are substantially better than the run times using CPLEX (column 4).

Table 2 is summarized with a cumulative distribution plot in Figure 6. Clearly, Figure 6(a) indicates that AMP is better able to find solutions within a 0.4% optimality gap (even without tuning). Figure 6(b) provides evidence of the overall strength of AMP. Even when AMP is not the fastest approach, its run times are very similar to BARON. Overall, the performance of AMP is clearly better using Gurobi as the underlying MILP/MIQCQP solver. We did not perform comparative studies of BARON with Gurobi because it cannot currently integrate with Gurobi.

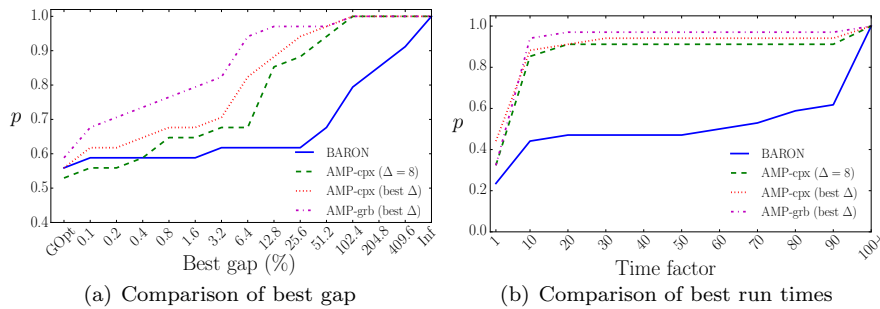


Fig. 6 Performance profiles of AMP (without bound-tightening) and BARON. In (a), the x axis plots the optimality gap of the algorithms and the y axis plots fraction of instances. Plot (a) tracks the number of instances where an algorithm is able achieve the specified optimality gap. In (b), the x axis denotes the run time ratio of an algorithm with the best run time of any algorithm. The y axis denotes the fraction of instances. Plot (b) tracks the number of times an algorithm’s run time is within a specified factor of the best run time of any algorithm. In both figures, higher is better. Overall, AMP performs better than BARON on a p proportion of instances for most gaps and all run times.

4.3 Performance of AMP with Bound-Tightening

We next discuss the performance of AMP when bound-tightening is added.

4.3.1 Default Parameters of Δ

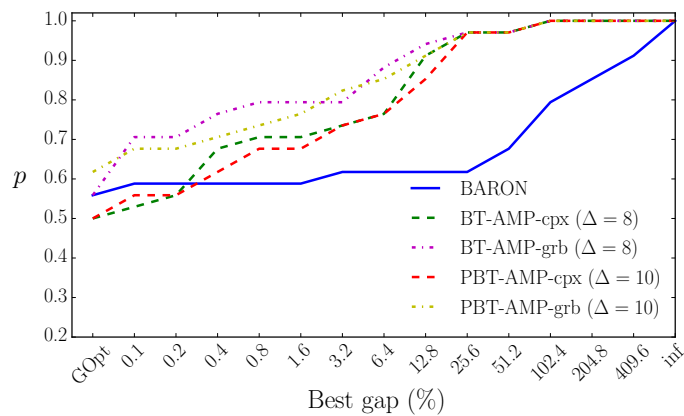
We first consider AMP with bound-tightening when AMP uses the default parameter of $\Delta = 8$. Table 3, compares AMP algorithm using CPLEX and Gurobi with BARON. Column two shows the run times of BARON based on a prescribed time limit. For comparison purposes with AMP, the time limit of BARON (T^+) is calculated as the sum of 3600 seconds and the maximum of the run time of BT and PBT. For the purposes of this study, we did not specify a time limit on BT and PBT, though this could be added.

Column three shows the performance of BT-AMP when $\Delta = 8$. While a constant Δ is not the ideal parameter for every instance, BT-AMP with CPLEX is still faster than BARON on 21 out of 32 instances. Similarly, BT-AMP with Gurobi is faster in 25 out of 32 instances. Once again, AMP with Gurobi has significant computational advantages over CPLEX. Instances *blend480*, *blend721*, *blend852*, and *meyer10* demonstrated an order of magnitude improvement. Column four of Table 3 shows the results of PBT-AMP when $\Delta = 10$. Though PBT solves a more complicated, discrete optimization problem at every step of bound-tightening, surprisingly, the total time spent in bound-tightening was typically significantly smaller. This is seen in all *ex...* instances, the *util* instance, the *eniplac* instance, the *meanvarx* instance and a few *blend* instances. In general, the tighter relaxations of PBT-AMP also yield significant improvements in the overall run times and optimality gaps of AMP.

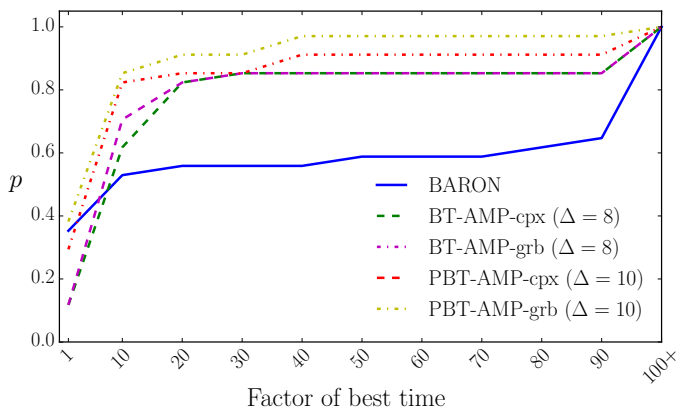
The bound-tightening also compares favorably with BARON. For example, consider problem *blend852*. Though BARON implements a sophisticated bound-tightening approach that is based on primal and dual formulations, BARON times out with a 0.08% gap. In contrast, BT-AMP with Gurobi converges to the global optimum in 434.7 seconds and PBT-AMP converges to the global optimum in 78.1 seconds (an order-of-magnitude improvement). Similar behaviour is observed on the remaining *blend*, *wts* and *meyer* instances. Overall, AMP with Gurobi outperforms BARON on 24 out of 32 instances when a default choice of Δ is used.

Table 3 is summarized with a cumulative distribution plot in Figure 7. Clearly, Figure 7(a) indicates that BT-AMP and PBT-AMP with Gurobi performs better than BARON even without tuning Δ . In 7(a), AMP has a better profile when the optimality gap is $> 0.4\%$. In Figure 7(a), the performance improvement starts at 0.2%. However, there is an increase in run times due to bound-tightening (Figure 7(b)), that allows to AMP to achieve this improvement.

Remark 2 *meyer15*, a generalized pooling problem-based instance, is classified as a large-scale MINLP and is very hard for global optimization. The current best known gap for this instance is 0.1% [37,8]. PBT-AMP with Gurobi has closed this problem by proving the *global optimum* for the first time (943734.0215–Table 3).



(a) Comparison of best gap



(b) Comparison of best run times

Fig. 7 Performance profiles of AMP (with bound-tightening) and BARON. In (a), the x axis plots the optimality gap of the algorithms and the y axis plots fraction of instances. Plot (a) tracks the number of instances where an algorithm is able achieve the specified optimality gap. In (b), the x axis denotes the run time ratio of an algorithm with the best run time of any algorithm. The y axis denotes the fraction of instances. Plot (b) tracks the number of times an algorithm’s run time is within a specified factor of the best run time of any algorithm. In both figures, higher is better. Overall, AMP performs better than BARON on p proportion of instances within a factor of the best gap and with the best run times.

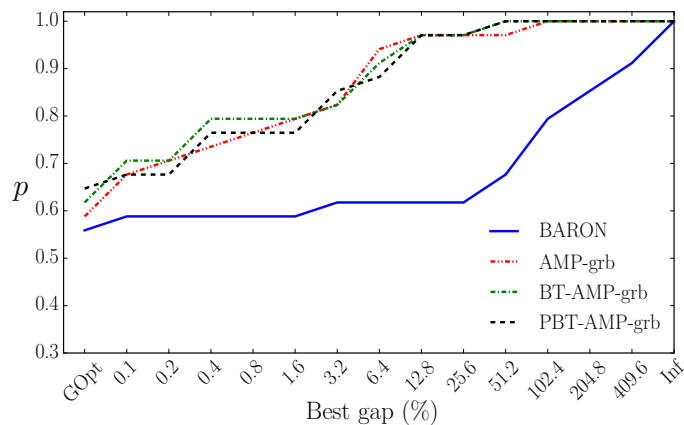
Table 3 Performance summary of AMP with bound-tightening on all instances. Here, we compare the run times of BARON, BT-AMP with $\Delta = 8$ and PBT-AMP with $\Delta = 10$. CPLEX and Gurobi are the underlying solvers for AMP. Values under “Gap” and “ T, T^+ ” are in % and seconds, respectively. “Inf” implies that the solver failed to provide a bound within the prescribed time limit.

Instances	BARON		BT	AMP-cpx		AMP-grb		PBT	AMP-cpx		AMP-grb	
	Gap	T^+	T^+	Gap	T	Gap	T	T^+	Gap	T	Gap	T
fuel	GOpt	0.03	0.01	GOpt	0.03	GOpt	0.03	0.01	GOpt	0.04	GOpt	0.03
ex1223a	GOpt	0.02	19.71	GOpt	0.01	GOpt	0.01	0.30	GOpt	0.01	GOpt	0.02
ex1264	GOpt	1.44	12.47	GOpt	1.77	GOpt	1.32	0.72	GOpt	1.48	GOpt	1.24
ex1265	GOpt	13.3	6.02	GOpt	0.25	GOpt	0.88	1.02	GOpt	0.26	GOpt	0.74
ex1266	GOpt	10.81	13.75	GOpt	0.12	GOpt	0.06	1.30	GOpt	0.04	GOpt	0.06
eniplac	GOpt	207.37	16.04	GOpt	1.13	GOpt	1.36	3.34	GOpt	1.17	GOpt	1.59
util	GOpt	0.10	9.92	GOpt	0.17	GOpt	0.19	0.61	GOpt	0.14	GOpt	0.16
meanvarx	GOpt	0.05	20.69	GOpt	95.23	GOpt	59.33	3.53	GOpt	13.62	GOpt	13.31
blend029	GOpt	2.46	15.05	GOpt	1.04	GOpt	1.56	0.80	GOpt	0.88	GOpt	0.95
blend531	GOpt	111.79	44.67	GOpt	38.60	GOpt	22.56	477.94	GOpt	39.89	GOpt	20.12
blend146	2.20	TO	30.95	24.92	TO	0.10	TO	26.66	24.98	TO	23.69	TO
blend718	175.10	TO	28.76	GOpt	1332.66	GOpt	1335.93	20.8	14.65	TO	GOpt	868.14
blend480	GOpt	326.95	137.62	0.21	TO	GOpt	108.93	1699.18	8.78	TO	GOpt	2466.17
blend721	GOpt	548.9	29.44	GOpt	646.92	GOpt	181.88	23.92	GOpt	93.28	GOpt	112.91
blend852	0.08	TO	41.73	GOpt	749.03	GOpt	392.99	29.40	GOpt	217.62	GOpt	48.79
wtsM2_05	GOpt	153.30	14.82	0.24	TO	0.02	TO	0.34	0.22	TO	GOpt	2875.17
wtsM2_06	GOpt	228.18	15.52	0.01	TO	0.01	TO	0.33	0.02	TO	GOpt	1957.59
wtsM2_07	GOpt	759.96	16.15	0.26	TO	0.30	TO	0.22	0.04	TO	1.59	TO
wtsM2_08	388.62	TO	21.54	14.37	TO	14.72	TO	0.90	20.08	TO	19.94	TO
wtsM2_09	Inf	TO	42.28	61.99	TO	64.53	TO	13.96	56.72	TO	55.85	TO
wtsM2_10	76.48	TO	15.73	0.10	TO	0.07	TO	0.32	0.22	TO	0.22	TO
wtsM2_11	107.56	TO	22.64	9.76	TO	3.74	TO	1.09	13.81	TO	9.18	TO
wtsM2_12	85.35	TO	39.10	11.90	TO	11.92	TO	3.44	6.03	TO	11.02	TO
wtsM2_13	54.04	TO	111.39	2.01	TO	3.95	TO	17.00	2.17	TO	2.10	TO
wtsM2_14	46.24	TO	19.09	6.64	TO	4.71	TO	1.10	1.93	TO	1.93	TO
wtsM2_15	Inf	TO	14.93	0.29	TO	0.50	TO	0.34	0.51	TO	0.48	TO
wtsM2_16	47.77	TO	22.54	8.76	TO	6.91	TO	1.18	9.40	TO	5.11	TO
lee1	GOpt	145.55	13.28	GOpt	12.50	GOpt	13.55	0.22	10.00	TO	0.01	TO
lee2	GOpt	590.08	14.92	0.58	TO	0.37	TO	5.35	0.43	TO	0.07	TO
meyer4	80.40	TO	15.78	GOpt	4.22	GOpt	4.47	238.47	GOpt	14.76	GOpt	13.68
meyer10	239.70	TO	44.68	9.74	TO	GOpt	2925.36	63.79	GOpt	TO	GOpt	1189.71
meyer15	2556.37	TO	3877.09	3.44	TO	0.08	TO	17868.96	GOpt	TO	GOpt	TO

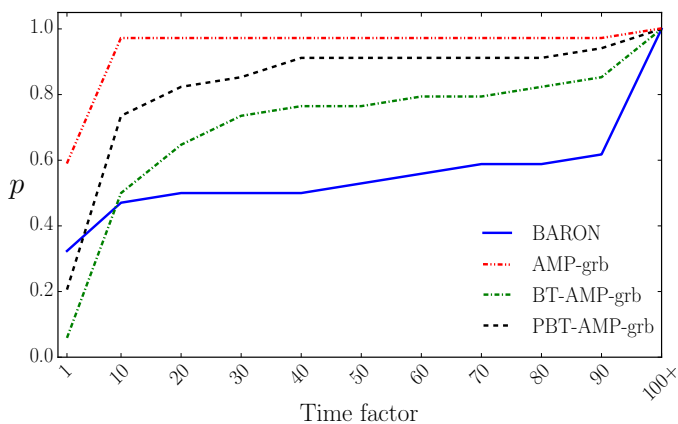
4.3.2 Tuned Parameters

In Table 4, we show the results of AMP (with bound-tightening) when Δ is tuned for each problem instance and these results are compared with BARON. As the performance of AMP is consistently the strongest with Gurobi, we present those results. Overall, this table shows the best results for AMP. Column two of this table shows the run times of BARON. Similar to table 3, the time limit for BARON (indicated as T^+) is the sum of 3600 seconds and the maximum of the run times of the BT and PBT algorithms (no time limit on BT and PBT). Column three tabulates the performance of BT-AMP with Gurobi by choosing the best Δ parameter for each instance. Overall, BT-AMP and PBT-AMP performed better than BARON on 26 out of 32 instances. As discussed in detail in section 4.3.1, similar observations about the performance of our algorithms also hold for this table. Again, the performance of PBT, despite the use of discrete optimization, indicates that PBT is the strongest bound-tightening procedure. On the large MINLP instance *meyer15*, PBT has large computational overhead, but this overhead pays off when AMP converges to the global optimum in 538.56 seconds. As noted in the earlier remark, this was an open instance prior to this work.

Table 3 is summarized with the cumulative distribution plot shown in Figure 8. Figure 8(a) indicates that AMP, BT-AMP and PBT-AMP with Gurobi are better than BARON in finding the best lower bounds. Though the proportion of instances for which global optima are attained is not significantly different than BARON, the proportion of instances for which better lower bounds are found using AMP-based algorithms is larger. Also, the advantages of BT and PBT-based bound-tightening in AMP is evident from the fact that the proportion of instances that find global optimum is higher. As expected, Figure 8(b) suggests that AMP with Gurobi is overall faster than BARON on the easiest instances, but on harder instances this speed is tempered by a degradation in solution quality.



(a) Comparison on Best Gap %



(b) Comparison on Best CPU Times

Fig. 8 Performance profiles of AMP (with bound-tightening and tuned Δ) and BARON. In (a), the x axis plots the optimality gap of the algorithms and the y axis plots fraction of instances. Plot (a) tracks the number of instances where an algorithm is able achieve the specified optimality gap. In (b), the x axis denotes the run time ratio of an algorithm with the best run time of any algorithm. The y axis denotes the fraction of instances. Plot (b) tracks the number of times an algorithm's run time is within a specified factor of the best run time of any algorithm. In both figures, higher is better. Overall, AMP-based algorithms perform better than BARON on p proportion of instances within a factor of the best gap and with the best run times.

Table 4 Summary of the performance of AMP with and without bound-tightening on all instances. Here, we compare the run times of BARON, BT-AMP and PBT-AMP with tuned values of Δ for each instance. Values under “Gap” and “ T, T^+ ” are in % and seconds, respectively. “Inf” implies that the solver failed to provide a bound within the prescribed time limit. Gap values shown within parenthesis are evaluated using global optimum values instead of the best-found upper bound by AMP.

Instances	BARON		BT-AMP-grb				PBT-AMP-grb			
	Gap	T^+	Δ^*	Gap	T^+	T	Δ^*	Gap	T^+	T
fuel	GOpt	0.03	8	GOpt	0.01	0.04	8	GOpt	0.01	0.04
ex1223a	GOpt	0.02	8	GOpt	19.71	0.01	32	GOpt	0.31	0.01
ex1264	GOpt	1.44	4	GOpt	12.47	0.59	4	GOpt	0.84	0.49
ex1265	GOpt	13.30	16	GOpt	6.02	0.45	16	GOpt	0.92	0.46
ex1266	GOpt	10.81	8	GOpt	13.75	0.06	4	GOpt	1.18	0.09
eniplac	GOpt	207.37	32	GOpt	16.04	0.45	32	GOpt	3.34	0.64
util	GOpt	0.10	4	GOpt	9.92	0.08	4	GOpt	0.56	0.09
meanvarx	GOpt	0.05	16	GOpt	20.69	21.17	16	GOpt	3.45	15.57
blend029	GOpt	2.46	32	GOpt	15.05	0.92	16	GOpt	1.09	1.33
blend531	GOpt	111.79	8	GOpt	44.67	22.56	32	GOpt	239.17	84.97
blend146	2.20	TO	8	0.10	30.95	TO	8	2.10	23.06	TO
blend718	175.10	TO	32	GOpt	28.76	889.28	8	GOpt	21.80	1101.56
blend480	GOpt	326.95	8	GOpt	137.62	108.93	16	GOpt	948.27	2185.03
blend721	GOpt	548.90	16	GOpt	29.44	92.27	32	GOpt	9.87	90.91
blend852	0.08	TO	16	GOpt	41.73	323.86	16	GOpt	14.16	323.31
wtsM2_05	GOpt	153.30	16	GOpt	14.82	2482.73	16	GOpt	0.33	2483.36
wtsM2_06	GOpt	228.18	16	GOpt	15.52	2058.92	16	GOpt	0.39	2057.20
wtsM2_07	GOpt	759.96	8	0.30	16.15	TO	8	0.30	0.24	TO
wtsM2_08	388.62	TO	4	8.25	21.54	TO	4	8.25	24.43	TO
wtsM2_09	Inf	TO	16	44.57	42.80	TO	16	43.66	288.88	TO
wtsM2_10	76.48	TO	8	0.07	15.73	TO	8	0.06	0.39	TO
wtsM2_11	107.56	TO	8	3.74	22.64	TO	8	2.39	1.11	TO
wtsM2_12	85.35	TO	4	(6.89) 7.29	39.10	TO	8	(6.95) 7.34	3.70	TO
wtsM2_13	54.04	TO	8	3.95	111.39	TO	4	6.92	130.31	TO
wtsM2_14	46.24	TO	32	2.71	19.09	TO	8	2.25	0.67	TO
wtsM2_15	Inf	TO	32	0.20	14.93	TO	16	0.28	0.35	TO
wtsM2_16	47.77	TO	4	(2.61) 5.81	22.54	TO	4	(3.04) 6.24	24.41	TO
lee1	GOpt	145.55	8	GOpt	13.28	13.55	8	GOpt	0.27	13.68
lee2	GOpt	590.08	16	0.36	14.92	TO	4	0.38	2.96	TO
meyer4	80.40	TO	8	GOpt	15.78	4.47	4	GOpt	77.61	8.45
meyer10	239.70	TO	4	GOpt	44.68	760.36	4	GOpt	34.67	775.74
meyer15	2556.37	TO	4	0.02	3877.09	TO	4	GOpt	19218.84	538.56

4.4 Sensitivity of MINLP structure

In Figure 9, we classify the MINLP instances to understand how problem structure influences the success of AMP. There are various possible classification measures and we use the total number of variables that are part of multi-linear terms. This is because our algorithm heavily depends on multi-variate partitioning on the nonlinear terms. Thus, it is likely that a measure like this influences the performance of AMP. Consider the following simple example that describes the measure clearly: Let $x_i, \forall i = 1, \dots, n$ be the variables in a problem with a linear objective and one nonlinear constraint, $\left(\prod_{i=1}^k x_i + \prod_{i=2}^{k+1} x_i\right) \geq M$, such that $2 \leq k \leq n - 1$. Then, the number of variables in multi-linear terms is $k + 1$.

It is clear from the figure that both AMP and BT-AMP performs very well on instances that have large numbers of variables (≥ 25) in the multi-linear terms. We also observe that while executing bound-tightening incurs a computational overhead (ratio up to ≈ 16), there are many instances below the unit ratio value (blue dashed line). Overall, these plots support the observation that increasing numbers of variables in multi-linear terms are indicator of success when executing AMP.

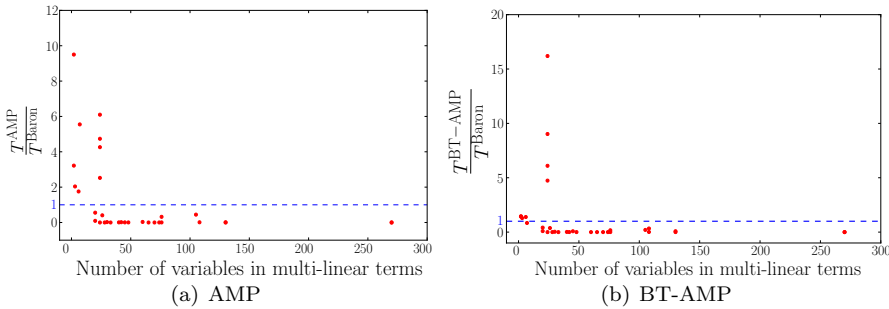


Fig. 9 Illustration of the ratio of run times of AMP and BT-AMP algorithms (with tuned parameters) to BARON. The y axis denotes the ratio and the x axis denotes the total number of variables in multi-linear terms in a given MINLP instance. The blue dashed line indicates a ratio of 1. All red points correspond to a single instance. A point below the blue line indicates a ratio in favor of AMP.

4.5 Bound-Tightening Results for *meyer15*

One of the primary observations made in this paper is the importance of MIP-based sequential bound-tightening on medium-scale MINLPs. However, for a given large-scale MINLP, one of the drawbacks of BT and PBT is that it solves MILPs to tighten the variable bounds. Solving MILPs can be time consuming,

in particular on instances like *meyer15*⁵. Here, we focus on the run time issues associated with solving MILPs, suggest approaches for managing that run time and still get much of their benefits in bound-tightening.

Table 5 summarizes the run times of BT and PBT on *meyer15* for various values of Δ . As shown in the first row of this table, the run time varies drastically when the MILP is solved to optimality in every iteration of BT and PBT. To reduce this run time, we imposed a time limit on every min- and max-MILP of *ten seconds*. Since early termination of MILP does not guarantee optimal primal-feasible solutions, incumbent solutions are not valid for bound-tightening. Instead, we use the best lower bound maintained by the solver. This ensures the validity of the tightened bounds. As shown in the second row of Table 5, the run times of PBT are drastically reduced.

Table 6 summarizes the results of AMP based on the tightened variable bounds presented in Table 5. Interestingly, on *meyer15*, we observed that AMP converges to near optimal solutions (sometimes, even better than solving full MILPs) when the time limit on MILP solvers is imposed. This is an important feature for tuning the time spent tightening bounds vs bound solution quality. Further, this intriguing result suggests further study of MILP-based relaxations for bound-tightening of MINLPs, which we delegate for future work.

Table 5 BT and PBT run times on *meyer15* with and without a limit on the run time of every MILP solved during the bound-tightening phase. Here, a 10-second time limit was used. The imposition of this limit reduces the total run time of PBT to close to BT.

	BT	PBT				
		$\Delta = 4$	$\Delta = 8$	$\Delta = 10$	$\Delta = 16$	$\Delta = 32$
Without time limit	3877	19218	32130	29586	11705	17868
With time limit	3830	3914	4059	4014	3635	3621

Table 6 AMP run times on *meyer15* instance preceded by bound-tightening with (BT-lim, PBT-lim) and without limit (BT, PBT) on run time per iteration. Values under “Gap” and “T” are in % and seconds, respectively. Bold font represents the best result in each row.

	$\Delta = 4$		$\Delta = 8$		$\Delta = 10$		$\Delta = 16$		$\Delta = 32$	
	Gap	T	Gap	T	Gap	T	Gap	T	Gap	T
After BT	0.02	TO	0.08	TO	0.12	TO	0.31	TO	0.15	TO
After BT-lim	0.37	TO	0.14	TO	0.17	TO	0.69	TO	0.90	TO
After PBT	GOpt	536.56	GOpt	1600	GOpt	TO	0.20	TO	0.15	TO
After PBT-lim	0.37	TO	0.90	TO	0.19	TO	0.70	TO	0.90	TO

⁵ *meyer15* is a generalized pooling problem instance. These problems are typically considered a hard (bilinear) MINLP for global optimization [37, 8]

Table 7 Overall structure of the MINLP problems. The first column describes the name of the problem instance. The second column cites the source of the problem. The third column shows the optimal solution. The fourth, fifth and sixth columns show the number of constraints, binary variables, and continuous variables, respectively. The seventh column indicates the partitioned continuous variables. “ALL” refers to all variables in multi-linear terms and “VC” refers to variables in the minimum vertex cover as described in [7]. The final column shows the number of multi-linear terms.

Instance	Ref.	GOpt	#Cons	#BVars	#CVars	#CVars-P	#ML
NLP1	[39]	7049.248	14	0	8	ALL	5
fuel	[8]	8566.119	15	3	12	VC	3
ex1223a	[8]	4.580	9	4	3	VC	3
ex1264	[8]	8.6	55	68	20	VC	16
ex1265	[8]	10.3	74	100	30	VC	25
ex1266	[8]	16.3	95	138	42	VC	36
eniplac	[8]	-132117.083	189	24	117	VC	66
util	[8]	999.578	167	28	117	ALL	5
meanvarx	[8]	14.369	44	14	21	VC	28
blend029	[8]	13.359	213	36	66	VC	28
blend531	[8]	20.039	736	104	168	VC	146
blend146	[8]	45.297	624	87	135	VC	104
blend718	[8]	7.394	606	87	135	VC	100
blend480	[8]	9.227	884	124	188	VC	152
blend721	[8]	13.5268	627	87	135	VC	104
blend852	[8]	53.9626	2412	120	184	VC	152
wtsM2.05	[36]	229.7008	152	0	134	VC	48
wtsM2.06	[36]	173.4784	152	0	134	VC	48
wtsM2.07	[36]	80.77892	152	0	134	VC	48
wtsM2.08	[36]	109.4014	335	0	279	VC	84
wtsM2.09	[36]	124.4421	573	0	517	ALL	210
wtsM2.10	[36]	586.68	138	0	156	VC	60
wtsM2.11	[36]	2127.115	252	0	304	VC	112
wtsM2.12	[36]	1201.038	408	0	517	VC	220
wtsM2.13	[36]	1564.958	783	0	1040	VC	480
wtsM2.14	[36]	513.009	205	0	209	VC	90
wtsM2.15	[36]	2446.429	152	0	134	VC	48
wtsM2.16	[36]	1358.663	234	0	244	VC	126
lee1	[35]	-4640.0824	82	9	40	VC	24
lee2	[35]	-3849.2654	92	9	44	VC	36
meyer4	[35]	1086187.137	118	55	63	VC	48
meyer10	[35]	1086187.137	423	187	207	VC	300
meyer15	[35]	943734.0215	768	352	382	VC	675

5 Conclusions

In this work, we developed an approach for adaptively partitioning non-convex functions in MINLPs. We show that an adaptive partitioning of the domains of variables outperforms uniform partitioning though the latter exhibits better optimality gaps in the first few iterations of the lower-bounding algorithm. We also show that bound-tightening techniques can be applied in conjunction with adaptive partitioning to improve convergence dramatically. We then used combinations of these techniques to develop an algorithm for solving MINLPs to global optimality. Our numerical experiments on MINLPs with multi-linear terms suggests that this is a very strong approach with an advantage of having very few tuning parameters in contrast to the existing methods.

We have seen that using adaptive piecewise polyhedral outer-approximations is an attractive way of tackling MINLPs. With an a priori fixed tolerance, we

get globally optimum solutions by utilizing the well-developed state-of-the-art MILP solvers. However, though AMP is relatively faster than the available global solvers, we observed that the computation times remain large for MINLPs with large number of multi-linear terms, thus motivating a multitude of directions for further developments. First, it will be important to consider existing classical nonlinear programming techniques, such as dual-based bound-contraction, partition elimination within the branch-and-bound search tree, bound-tightening at sub nodes [38], and constraint propagation methods [3], which can tremendously speed-up our algorithm. Second, an important direction develops apriori guarantees on the size of the added partitions (Δ) that leads to faster tightening of the relaxations. This will support automatic tuning of Δ from within AMP. Third, recent developments on generating tight convex hull-reformulation-based cutting planes for solving convex generalized disjunctive programs will be very effective for attaining faster convergence to global optimum [52]. Finally, extensions of our methods from multi-linear to general non-convex functions (including fractional exponents, transcendental functions, disjunctions of non-convex functions [44], etc.) will be another direction that will have relevance to numerous practical applications.

References

1. Achterberg, T.: Scip: solving constraint integer programs. *Mathematical Programming Computation* **1**(1), 1–41 (2009)
2. Al-Khayyal, F.A., Falk, J.E.: Jointly constrained biconvex programming. *Mathematics of Operations Research* **8**(2), 273–286 (1983)
3. Belotti, P.: Bound reduction using pairs of linear inequalities. *Journal of Global Optimization* **56**(3), 787–819 (2013)
4. Belotti, P., Cafieri, S., Lee, J., Liberti, L.: On feasibility based bounds tightening (2012). URL <https://hal.archives-ouvertes.fr/file/index/docid/935464/filename/377.pdf>
5. Belotti, P., Lee, J., Liberti, L., Margot, F., Wächter, A.: Branching and bounds tightening techniques for non-convex minlp. *Optimization Methods & Software* **24**(4-5), 597–634 (2009)
6. Bergamini, M.L., Grossmann, I., Scenna, N., Aguirre, P.: An improved piecewise outer-approximation algorithm for the global optimization of MINLP models involving concave and bilinear terms. *Computers & Chemical Engineering* **32**(3), 477–493 (2008)
7. Boukouvava, F., Misener, R., Floudas, C.A.: Global optimization advances in mixed-integer nonlinear programming, minlp, and constrained derivative-free optimization, cdfo. *European Journal of Operational Research* **252**(3), 701–727 (2016)
8. Bussieck, M.R., Drud, A.S., Meeraus, A.: MINLPLib—a collection of test models for mixed-integer nonlinear programming. *INFORMS Journal on Computing* **15**(1), 114–119 (2003)
9. Cafieri, S., Lee, J., Liberti, L.: On convex relaxations of quadrilinear terms. *Journal of Global Optimization* **47**(4), 661–685 (2010)
10. Carothers, N.L.: *Real analysis*. Cambridge University Press (2000)
11. Castro, P.M.: Normalized multiparametric disaggregation: an efficient relaxation for mixed-integer bilinear problems. *Journal of Global Optimization* pp. 1–20 (2015)
12. Castro, P.M.: Tightening piecewise McCormick relaxations for bilinear problems. *Computers & Chemical Engineering* **72**, 300–311 (2015)
13. Castro, P.M., Grossmann, I.E.: Optimality-based bound contraction with multiparametric disaggregation for the global optimization of mixed-integer bilinear problems. *Journal of Global Optimization* **59**(2-3), 277–306 (2014)

14. Coffrin, C., Hijazi, H.L., Van Hentenryck, P.: Strengthening convex relaxations with bound tightening for power network optimization. In: Principles and Practice of Constraint Programming, pp. 39–57. Springer (2015)
15. Dunning, I., Huchette, J., Lubin, M.: Jump: A modeling language for mathematical optimization. *SIAM Review* **59**(2), 295–320 (2017)
16. D’Ambrosio, C., Lodi, A., Martello, S.: Piecewise linear approximation of functions of two variables in milp models. *Operations Research Letters* **38**(1), 39–46 (2010)
17. Faria, D.C., Bagajewicz, M.J.: Novel bound contraction procedure for global optimization of bilinear MINLP problems with applications to water management problems. *Computers & chemical engineering* **35**(3), 446–455 (2011)
18. Grossmann, I.E., Trespalacios, F.: Systematic modeling of discrete-continuous optimization models through generalized disjunctive programming. *AIChE Journal* **59**(9), 3276–3295 (2013)
19. Gupte, A., Ahmed, S., Cheon, M.S., Dey, S.: Solving mixed integer bilinear problems using MILP formulations. *SIAM Journal on Optimization* **23**(2), 721–744 (2013)
20. Hasan, M., Karimi, I.: Piecewise linear relaxation of bilinear programs using bivariate partitioning. *AIChE journal* **56**(7), 1880–1893 (2010)
21. Hijazi, H.: Perspective envelopes for bilinear functions (2015). URL www.optimization-online.org/DB_FILE/2015/03/4841.pdf
22. Hijazi, H., Coffrin, C., Hentenryck, P.V.: Convex quadratic relaxations for mixed-integer nonlinear programs in power systems. *Mathematical Programming Computation* pp. 1–47 (2016)
23. Hock, W., Schittkowski, K.: Test examples for nonlinear programming codes. *Journal of Optimization Theory and Applications* **30**(1), 127–129 (1980)
24. Horst, R., Pardalos, P.M.: Handbook of global optimization, vol. 2. Springer Science & Business Media (2013)
25. Kannan, R., Monma, C.L.: On the computational complexity of integer programming problems. In: Optimization and Operations Research, pp. 161–172. Springer (1978)
26. Karuppiah, R., Grossmann, I.E.: Global optimization for the synthesis of integrated water systems in chemical processes. *Computers & Chemical Engineering* **30**(4), 650–673 (2006)
27. Kocuk, B., Dey, S.S., Sun, X.A.: Strong socp relaxations for the optimal power flow problem. *Operations Research* **64**(6), 1177–1196 (2016)
28. Kolodziej, S.P., Grossmann, I.E., Furman, K.C., Sawaya, N.W.: A discretization-based approach for the optimization of the multiperiod blend scheduling problem. *Computers & Chemical Engineering* **53**, 122–142 (2013)
29. Li, H.L., Huang, Y.H., Fang, S.C.: A logarithmic method for reducing binary variables and inequality constraints in solving task assignment problems. *INFORMS Journal on Computing* **25**(4), 643–653 (2012)
30. Liberti, L., Lavor, C., Maculan, N.: A branch-and-prune algorithm for the molecular distance geometry problem. *International Transactions in Operational Research* **15**(1), 1–17 (2008)
31. Lu, M., Nagarajan, H., Yamangil, E., Bent, R., Backhaus, S.: Optimal transmission line switching under geomagnetic disturbances. arXiv preprint arXiv:1701.01469 (2017)
32. Luedtke, J., Namazifar, M., Linderoth, J.: Some results on the strength of relaxations of multilinear functions. *Mathematical programming* **136**(2), 325–351 (2012)
33. McCormick, G.P.: Computability of global solutions to factorable nonconvex programs: Part i—convex underestimating problems. *Mathematical programming* **10**(1), 147–175 (1976)
34. Meyer, C.A., Floudas, C.A.: Global optimization of a combinatorially complex generalized pooling problem. *AIChE journal* **52**(3), 1027–1037 (2006)
35. Misener Ruth, F.C.: Generalized pooling problem (2011). Available from Cyber-Infrastructure for MINLP [www.minlp.org, a collaboration of Carnegie Mellon University and IBM Research] at: www.minlp.org/library/problem/index.php?i=123
36. Misener, R., Floudas, C.A.: GloMIQO: Global mixed-integer quadratic optimizer. *Journal of Global Optimization* pp. 1–48 (2013)
37. Misener, R., Thompson, J.P., Floudas, C.A.: Apogee: Global optimization of standard, generalized, and extended pooling problems via linear and logarithmic partitioning schemes. *Computers & Chemical Engineering* **35**(5), 876–892 (2011)

38. Mouret, S., Grossmann, I.E., Pectiaux, P.: Tightening the linear relaxation of a mixed integer nonlinear program using constraint programming. In: *Integration of AI and OR Techniques in Constraint Programming for Combinatorial Optimization Problems*, pp. 208–222. Springer (2009)
39. Nagarajan, H., Lu, M., Yamangil, E., Bent, R.: Tightening McCormick relaxations for nonlinear programs via dynamic multivariate partitioning. In: *International Conference on Principles and Practice of Constraint Programming*, pp. 369–387. Springer (2016)
40. Nagarajan, H., Pagilla, P., Darbha, S., Bent, R., Khargonekar, P.: Optimal configurations to minimize disturbance propagation in manufacturing networks. In: *American Control Conference (ACC)*, 2017, pp. 2213–2218. IEEE (2017)
41. Nagarajan, H., Yamangil, E., Bent, R., Van Hentenryck, P., Backhaus, S.: Optimal resilient transmission grid design. In: *Power Systems Computation Conference (PSCC)*, 2016, pp. 1–7. IEEE (2016)
42. Puranik, Y., Sahinidis, N.V.: Domain reduction techniques for global NLP and MINLP optimization. *Constraints* **22**(3), 338–376 (2017)
43. Rikun, A.D.: A Convex Envelope Formula for Multilinear Functions. *Journal of Global Optimization* **10**, 425–437 (1997). DOI 10.1023/A:1008217604285
44. Ruiz, J.P., Grossmann, I.E.: Global optimization of non-convex generalized disjunctive programs: a review on reformulations and relaxation techniques. *Journal of Global Optimization* pp. 1–16 (2016)
45. Ryoo, H.S., Sahinidis, N.V.: Global optimization of nonconvex nlp and MINLPs with applications in process design. *Computers & Chemical Engineering* **19**(5), 551–566 (1995)
46. Ryoo, H.S., Sahinidis, N.V.: Analysis of bounds for multilinear functions. *Journal of Global Optimization* **19**(4), 403–424 (2001)
47. Sahinidis, N.V.: Baron: A general purpose global optimization software package. *Journal of global optimization* **8**(2), 201–205 (1996)
48. Smith, E.M., Pantelides, C.C.: A symbolic reformulation/spatial b&b algorithm for the global optimization of nonconvex MINLPs. *Computers & Chemical Engineering* **23**(4), 457–478 (1999)
49. Speakman, E.E.: *Volumetric Guidance for Handling Triple Products in Spatial Branch-and-Bound*. Ph.D. thesis, University of Michigan (2017)
50. Tawarmalani, M., Sahinidis, N.V.: A polyhedral branch-and-cut approach to global optimization. *Mathematical Programming* **103**(2), 225–249 (2005)
51. Teles, J.P., Castro, P.M., Matos, H.A.: Univariate parameterization for global optimization of mixed-integer polynomial problems. *European Journal of Operational Research* **229**(3), 613–625 (2013)
52. Trespacios, F., Grossmann, I.E.: Cutting plane algorithm for convex generalized disjunctive programs. *INFORMS Journal on Computing* **28**(2), 209–222 (2016)
53. Vielma, J.P., Nemhauser, G.L.: Modeling disjunctive constraints with a logarithmic number of binary variables and constraints. *Mathematical Programming* **128**(1), 49–72 (2011)
54. Wicaksono, D.S., Karimi, I.: Piecewise MILP under- and overestimators for global optimization of bilinear programs. *AIChE Journal* **54**(4), 991–1008 (2008)
55. Wu, F., Nagarajan, H., Zlotnik, A., Sioshansi, R., Rudkevich, A.: Adaptive convex relaxations for gas pipeline network optimization. In: *American Control Conference (ACC)*, 2017, pp. 4710–4716. IEEE (2017)

A Appendix

A.1 Sensitivity Analysis of Δ

One of the important details of MINLP algorithms and approaches is their parameterization. As seen in the earlier sections, AMP is no different. The quality of the solutions depend heavily on the choice of Δ . However, in spite of this problem specific dependence, it is often interesting to identify reasonable default values. Table 8 presents computational results on all instances for different choices of Δ . From these results, AMP is most effective when Δ is between 4 and 10.

Table 8 This table shows a sensitivity analysis of AMP’s performance to the choice of Δ . Here, we bin results by $\Delta \leq 4$, Δ between 4 and 10, and $\Delta > 10$. From these results, it is clear that most of the good choices of Δ are between 4 and 10 and this is our recommended choice for this parameter.

Instances	$\Delta \leq 4$		$4 < \Delta \leq 10$		$\Delta > 10$	
	Gap(%)	T	Gap(%)	T	Gap(%)	T
p1	GOpt	0.74	GOpt	0.24	GOpt	0.06
p2	GOpt	0.60	GOpt	0.20	GOpt	0.10
fuel	GOpt	0.05	GOpt	0.06	GOpt	0.07
ex1223a	GOpt	0.03	GOpt	0.02	GOpt	0.02
ex1264	GOpt	1.92	GOpt	0.79	GOpt	1.03
ex1265	GOpt	2.24	GOpt	0.28	GOpt	0.80
ex1266	GOpt	0.20	GOpt	0.23	GOpt	0.16
eniplac	GOpt	2.39	GOpt	1.46	GOpt	0.75
util	GOpt	2.52	GOpt	2.14	GOpt	0.55
meanvarx	GOpt	967.70	GOpt	118.80	GOpt	70.09
blend029	GOpt	1.98	GOpt	1.33	GOpt	1.00
blend531	GOpt	88.60	GOpt	74.33	GOpt	49.76
blend146	23.34	TO	1.60	TO	3.20	TO
blend718	GOpt	1263.41	GOpt	581.68	GOpt	889.72
blend480	0.10	TO	0.02	TO	0.02	TO
blend721	GOpt	486.17	GOpt	44.13	GOpt	176.11
blend852	0.01	TO	GOpt	144.26	GOpt	322.80
wtsM2_05	GOpt	2236.45	GOpt	2545.41	GOpt	386.95
wtsM2_06	0.02	TO	GOpt	519.38	GOpt	972.20
wtsM2_07	0.77	TO	0.57	TO	0.54	TO
wtsM2_08	7.92	TO	9.28	TO	11.96	TO
wtsM2_09	7.47	TO	68.58	TO	68.58	TO
wtsM2_10	0.11	TO	0.11	TO	0.10	TO
wtsM2_11	6.10	TO	6.27	TO	10.41	TO
wtsM2_12	6.49	TO	8.69	TO	4.00	TO
wtsM2_13	7.37	TO	2.03	TO	10.27	TO
wtsM2_14	4.06	TO	5.59	TO	1.43	TO
wtsM2_15	0.17	TO	0.17	TO	0.57	TO
wtsM2_16	5.73	TO	8.17	TO	5.25	TO
lee1	GOpt	73.19	GOpt	13.61	0.03	TO
lee2	0.38	TO	0.02	TO	0.08	TO
meyer4	GOpt	64.82	GOpt	5.33	GOpt	20.74
meyer10	GOpt	684.63	GOpt	133.47	9.70	TO
meyer15	0.10	TO	0.33	TO	0.15	TO
Summary		7		14		14

A.2 Logarithmic and Linear Encodings of Partition Variables

In section 2, the discussion on piece-wise convex relaxations described formulations that encoded the partition variables with a linear number of variables and a logarithmic number of variables (SOS-1 constraints). Table 9 compares the performance of AMP using both formulations. Despite fewer variables in the logarithmic formulation, this encoding is only effective on a few problems, generally on problems that require a significant number of partitions. These results suggest that when the logarithmic encoding has nearly the same number of partition variables as the linear encoding, the linear encoding is more effective.

Table 9 This table compares the logarithmic formulation of partition variables with the linear representation. Each column indicates the formulation with the fastest runtime for different choices of Δ . The last column enumerates the number of times the logarithmic formulation is better. On the smaller, easier instances the linear model is better, as the linear formulation preserves structure in the partition choices. However, as the problems get more difficult to solve (more partitions) the benefit of having fewer binary variables becomes more apparent.

Instances	$F(\Delta = 4)$	$F(\Delta = 8)$	$F(\Delta = 10)$	$F(\Delta = 16)$	$F(\Delta = 32)$	Total
eniplac	lin	lin	log	log	log	3
blend531	lin	lin	log	lin	lin	1
blend146	lin	lin	log	lin	lin	1
blend718	lin	lin	lin	lin	log	1
blend480	lin	lin	log	lin	lin	1
blend721	lin	lin	lin	lin	lin	0
blend852	log	lin	log	lin	log	3
wtsM2.05	lin	lin	lin	lin	lin	0
wtsM2.06	lin	lin	lin	lin	lin	0
wtsM2.07	lin	lin	lin	lin	lin	0
wtsM2.08	log	lin	log	lin	log	3
wtsM2.09	lin	log	log	log	log	4
wtsM2.10	lin	lin	lin	lin	lin	0
wtsM2.11	lin	lin	lin	lin	lin	0
wtsM2.12	lin	lin	lin	lin	lin	0
wtsM2.13	lin	lin	lin	lin	lin	0
wtsM2.14	lin	lin	lin	lin	lin	0
wtsM2.15	log	lin	lin	lin	log	2
wtsM2.16	lin	lin	lin	lin	lin	0
lee1	log	log	log	log	log	5
lee2	log	lin	lin	lin	lin	1
meyer4	log	log	lin	lin	log	3
meyer10	lin	lin	log	log	lin	2
meyer15	log	log	lin	lin	log	3
Total	7	4	9	5	8	33